AD-A164 162 EXPERIMENTAL STUDY OF ACTIVE VIBRATION CONTROL(U) 1/1
VIRGINIA POLYTECHNIC INST AND STATE UNIV BLACKSBURG
DEPT OF A W L HALLAUER ET AL 13 FEB 85
UNCLASSIFIED AFOSR-TR-85-1234 F49600-83-C-0158 F/G 20/11 NL

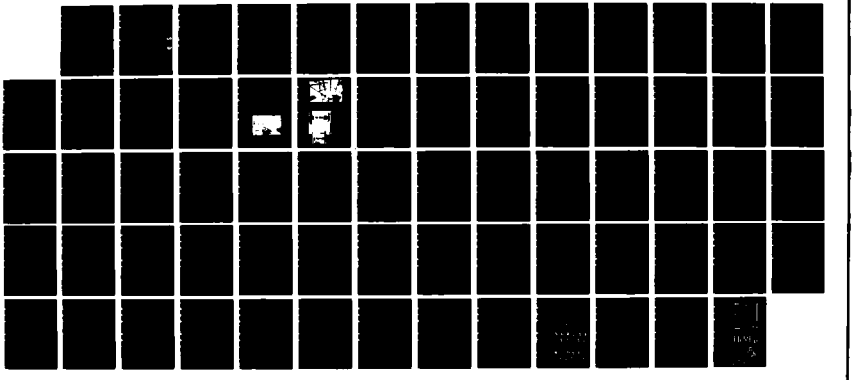

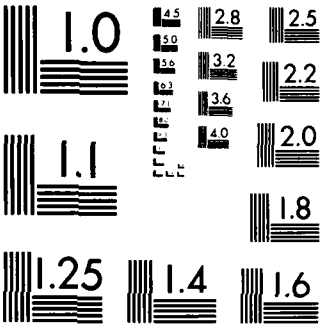

MICROCOPY RESOLUTION TEST CHART

NARDS-1963-A

(2)

SECURITY

AD-A164 162

DOCUMENTATION PAGE

1a. REPORT SECURITY CLASSIFICATION: Unclassified	1b. RESTRICTIVE MARKINGS
2a. SECURITY CLASSIFICATION AUTHORITY	3. DISTRIBUTION/AVAILABILITY OF REPORT: Unclassified/Unlimited for public release
2b. DECLASSIFICATION/DOWNGRADING SCHEDULE	
4. PERFORMING ORGANIZATION REPORT NUMBER(S)	5. MONITORING ORGANIZATION REPORT NUMBER(S): AFOSR-TR- 85-1234
6a. NAME OF PERFORMING ORGANIZATION: Virginia Polytechnic Institute and State University; 6b. OFFICE SYMBOL (If applicable): AOE	7a. NAME OF MONITORING ORGANIZATION: Air Force Office of Scientific Research/NA
6c. ADDRESS (City, State and ZIP Code): Dept. of Aerospace and Ocean Engineering, VPI & SU, Blacksburg, Virginia 24061	7b. ADDRESS (City, State and ZIP Code): Directorate of Aerospace Sciences, Building 410, Bolling AFB, DC 20332
8a. NAME OF FUNDING/SPONSORING ORGANIZATION: Air Force Office of Scientific Research; 8b. OFFICE SYMBOL (If applicable): AFOSR/NA	9. PROCUREMENT INSTRUMENT IDENTIFICATION NUMBER: Contract F49620-83-C-0158
8c. ADDRESS (City, State and ZIP Code): Bolling AFB DC 20332-6448	10. SOURCE OF FUNDING NOS.

PROGRAM ELEMENT NO.	PROJECT NO.	TASK NO.	WORK UNIT NO.
61102F	2307	B1	

11. TITLE (Include Security Classification): Experimental Study of Active Vibration Control

12. PERSONAL AUTHOR(S): Hallauer, William L. Jr. (VPI & SU); Nayak, Arun P. (Subcontractor HR Textron)

13a. TYPE OF REPORT	13b. TIME COVERED	14. DATE OF REPORT (Yr., Mo., Day)	15. PAGE COUNT
Final Technical	FROM 83-9-1 TO 84-12-31	1985, February 13	65

16. SUPPLEMENTARY NOTATION

17. COSATI CODES			18. SUBJECT TERMS (Continue on reverse if necessary and identify by block number)
FIELD	GROUP	SUB. GR.	Structural dynamics Active vibration damping (control) Experimental modal analysis

SELECTED FEB 13 1986 D

19. ABSTRACT (Continue on reverse if necessary and identify by block number)

Three different types of active vibration damping were implemented on a pendulous, two-dimensional laboratory structure having high modal density at low frequencies (0-10 Hz) and very light inherent damping. The most effective control system included an array processor (the controller) and five pairs of dual (colocated) velocity sensors and force actuators. This control system was used for implementation of two different active damping techniques, uncoupled and coupled rate feedback. The latter was based on modal-space active damping. Both techniques produced heavy active damping of eleven modes with natural frequencies under 10 Hz, and both positively augmented the damping of all modes. Both techniques were proven to be completely stable and stability-robust relative to errors in the structure theoretical model. Very good agreement was achieved between experimentally measured and theoretically calculated structure-control system dynamic response. The most significant result is that the technique of coupled rate feedback with dual sensors and actuators effectively damped many more modes than the number of control actuators while producing no spillover instability.

20. DISTRIBUTION/AVAILABILITY OF ABSTRACT	21. ABSTRACT SECURITY CLASSIFICATION
UNCLASSIFIED/UNLIMITED ☒ SAME AS RPT. ☐ OTIC USERS ☐	Unclassified

22a. NAME OF RESPONSIBLE INDIVIDUAL	22b. TELEPHONE NUMBER (Include Area Code)	22c. OFFICE SYMBOL
Anthony K. Amos	202/767-4937	AFOSR/NA

OTIC FILE COPY

DD FORM 1473, 83 APR EDITION OF 1 JAN 73 IS OBSOLETE. UNCLASSIFIED

SECURITY CLASSIFICATION OF THIS PAGE

FINAL TECHNICAL REPORT
TO THE AIR FORCE OFFICE OF SCIENTIFIC RESEARCH
FOR THE PERIOD 1 SEPTEMBER 1983 TO 31 DECEMBER 1984

CONTRACT F49620-83-C-0158

EXPERIMENTAL STUDY OF ACTIVE VIBRATION CONTROL*

William L. Hallauer Jr.
Department of Aerospace and Ocean Engineering
Virginia Polytechnic Institute and State University

TABLE OF CONTENTS

*Dr. Anthony Amos was the AFOSR Program Manager. This research is continuing with AFOSR sponsorship under Contract F49620-85-C-0024.

1. INTRODUCTION

The subject of this research was active vibration damping, with applications intended for future large space structures (LSS). The research included complementary experimental and theoretical studies. An important general objective was to achieve satisfactory agreement between experiment and theory, thus validating theoretical concepts for practical application or exposing the reasons why they are inapplicable or ineffective.

A substantial portion of the work was experimental, and it was conducted on Earth rather than in the weightlessness of space. In order for the research to be relevant to the dynamics and control of LSS, it was necessary to focus on appropriate laboratory equipment, including a structure and control devices.

The structure used was a pendulous assemblage of several different elements; it is illustrated in Figs. 1-4. It consisted of a highly flexible plane grid of aluminum beams, two rigid eccentric weights, and a steel top beam, which was supported in low friction bearings that permitted the entire assemblage to have a very low frequency, nearly rigid body pendulum mode. The pendulous structure was designed to have structural dynamics similar in as many respects as possible to those of future LSS. The structure did not have true rigid body modes, and it could not accommodate large rigid body rotation representative of slewing of a spacecraft. But it did have the important characteristic of relatively high modal density at low frequencies (in the 0-10 Hz range).

In contrast, the control system hardware used was not necessarily representative of that likely to be found on a LSS. Indeed, it is very

difficult at present to build a realistic laboratory simulation of a LSS vibration control system because very few hardware devices have been qualified for space application. The controller used in the experiments was a high speed, programmable array processor, shown in Fig. 2. The sensors, shown in Fig. 4, were noncontacting velocity measuring devices consisting of structure-borne conducting coils and externally supported magnetic field structures. The actuators were noncontacting force generators identical in form to the velocity sensors. Sensor operation was similar to that of a dynamic microphone, and actuator operation was similar to that of a dynamic loudspeaker.

The actuator magnetic field structures were externally supported rather than being borne by the vibrating structure. This was the most serious deficiency of the control system hardware relative to the objective of simulating a typical LSS control system. Moreover, the sensors and actuators essentially had no dynamics of their own; that is, their bandwidth of flat response was essentially infinite relative to the laboratory structure's low frequencies of interest. On the other hand, these devices did exhibit levels of electrical noise typical of standard control system sensing and actuating instruments.

Two general active damping approaches were studied, both involving only rate feedback. The approach studied in greatest detail is modal-space active damping; versions of this for two fundamentally different modal estimation (filtering) techniques were evaluated. The second approach studied is uncoupled (direct) rate feedback active damping.

This report is primarily a summary of the subject research. Most details relative to the first half (roughly) of the contract period are given in Ref. 1. Details relative to the second half of the contract period are given

in the appendices and/or will appear in technical papers presently being prepared. These future detailed papers are cited among the references.

2. RESEARCH OBJECTIVES

The primary specific objective of the work was active damping of a number of vibration modes greater than the number of control actuators. An important supporting objective was development of an effective method for estimating the responses of individual vibration modes. Two methods, bandpass spectral filtering and spatial filtering, were evaluated.

In the past, modes of the pendulous structure calculated by the finite element method did not agree satisfactorily with the measured modes. Therefore, another objective of this work was to achieve satisfactory agreement by appropriate modification of both the laboratory structure and its finite element model.

Subcontractor HR Textron supported this research with the specific objectives of conducting a review and critical analysis of VPI's work and using advanced theoretical techniques to design controllers for possible experimental implementation at VPI.

The final objective was to begin laboratory implementation of active vibration damping by means of a digital controller, rather than the analog controllers that were used previously.

3. ACCOMPLISHMENTS OF THE RESEARCH

3.1 SPECTRAL AND SPATIAL MODAL FILTERING

These techniques for estimating the responses of individual vibration modes were used in conjunction with modal-space active damping. Reference 1 describes in detail the dynamics of the bandpass spectral modal filters and demonstrates conclusively that they are unsuitable for their intended

function. The significant result, in summary, is: in order to avoid instability due to mode-filter coupling, the bandwidth of a spectral filter for a given controlled mode must be so narrow as to reject response from all other modes; but, by virtue of being so narrow, the bandwidth can reduce the effective active damping to such a low level as to be useless.

It has become clear that all types of spectral filtering, not just bandpass filtering, can cause unexpected difficulties if applied to active vibration damping. The dynamics of spectral filters inevitably influence system dynamics. Consider, as perhaps the best example, use of a lowpass spectral filter to eliminate high frequency content from sensor signals in an attempt to prevent observation spillover. A lowpass filter is generally considered to be a benign device, but it is indeed benign only if the phase lag it induces is not important. However, phases are extremely important in feedback control, and even simple one-pole and two-pole lowpass filters introduce significant phase lags. So spectral filtering should be applied very cautiously, if at all, to active vibration damping.

The most appropriate simple alternative to bandpass spectral modal filtering is a technique called spatial modal filtering (Ref. 2) or static observation (Ref. 3), and this technique was adopted after spectral filtering proved unsatisfactory. The practical disadvantage of spatial filtering is that it requires a large number of motion sensors, whereas spectral filtering requires, in principle, only one sensor. Therefore, it was necessary to fabricate and calibrate the additional sensors required for spatial filtering, and to replace spectral filtering with spatial filtering in all theoretical modeling. Several additional velocity sensors were fabricated, a special-purpose calibration frame was designed and fabricated, and all the additional sensors were mounted on the laboratory structure. Revision of the

theoretical model in computer coding was completed, and computer simulations were run to provide guidance in the choice of sensor numbers and locations for the hardware experiments.

Difficulties arose even with spatial modal filtering. The results of several computer simulations showed that this method of modal estimation frequently produces spillover instability in residual (uncontrolled) modes. No instability occurs if the sensors are dual* with the actuators, but, contrary to intuition, increasing the number of sensors beyond the number of actuators inevitably produces instability in at least one of the residual modes. For this reason, spatial filtering was implemented only for sensors dual with actuators.

3.2 PENDULOUS LABORATORY STRUCTURE

This structure was designed to be dynamically representative in many respects of a flexible satellite structure. The hardware has been modified considerably since initial fabrication, resulting in improved dynamic response relative to the objectives of this research. The design and fabrication are summarized in Ref. 1 and described in great detail in Refs. 4 and 5.

The finite element model of the structure also has gone through a great deal of refinement in the quest to calculate modes that match well with measured modes. Despite this refinement, the most recent reports (Refs. 1 and 5) show that the calculated mode shape of the second mode was considerably different from the measured mode shape, and that empiricism was required to make the calculated frequency of the fundamental mode (a simple pendulum mode!) match the measured frequency.

Subsequent to completion of those reports, the reason was determined

---

*The word "dual" is used rather than the more common but less precise "colocated". "Dual" implies that a sensor and actuator are not only colocated but also coaxial, and that they act in the same discrete degree of freedom.

for the perplexing failure of the finite element model to predict accurately the first and second modes, and the model was revised accordingly. Essentially, the previous model did not account for all the effects of gravity. The revision consisted of implementation of an element geometric stiffness matrix (Ref. 6) that accounts correctly for gravity. A paper is being prepared for publication which will describe in detail the design and theoretical and experimental analyses of the pendulous structure (Ref. 7).

The lowest twenty natural frequencies calculated from the revised finite element model are listed in Table 1 (under Open-Loop Roots). These results are for a 58-DOF model. The first twelve of the calculated frequencies agree very well (within a few percent) with the measured natural frequencies. Also shown in Table 1 are the modal inherent viscous damping factors used in the theoretical model of the pendulous structure for the active damping studies. The first thirteen inherent damping factors were measured experimentally.

3.3 ACTIVE DAMPING RESULTS

The results for modal-space active damping with spectral modal filtering are summarized in Section 3.1 and reported in detail in Ref. 1.

Another version of modal-space active damping was studied since the first version proved unsuccessful. The second version uses spatial modal filtering with dual sensors and actuators. The complete theory behind this approach is presented in Appendix A. The technique not only is stable, but also produces substantial active damping in several of the residual modes. Since the number of controlled modes is equal to the number of actuators, it is clear that this technique achieves the objective of actively damping more modes that there are actuators. As is shown in Appendix A, this technique involves a fully populated matrix of feedback gains that includes terms coupling every velocity sensor with every force actuator; therefore, it is

referred to as "coupled rate feedback."

This coupled rate feedback was evaluated experimentally and theoretically for the pendulous laboratory structure and with the following conditions. Velocity sensors and force actuators were located at joints 1, 2, 4, 5, and 8 (see Fig. 1). Modes 2-6 were designated as the controlled modes, and it was specified that the desired modal active damping factor of each be 0.1. The damping factors actually achieved (based on a 20-mode theoretical model -- see Appendix A) are listed in Table 1. Damping factors achieved for the controlled modes were close to the desired values, and the damping of every residual mode was positively augmented. In particular, with the exception of modes 7 and 8 (very low level modes of the steel top beam), all modes with natural frequencies under 10 Hz received significant active damping. This excellent performance is especially evident in the experimental and theoretical frequency response functions of Figs. 5 and 6. These figures are representative of many frequency response functions that have been evaluated.

For comparison with coupled rate feedback, a form of uncoupled (direct) rate feedback also was studied. This technique is comparable to providing a viscous dashpot at each sensor-actuator degree of freedom. It involves a diagonal (uncoupled) matrix of feedback gains, which means that each actuator receives feedback signals only from its own dual sensor.

A linear programming method for choosing the gains is developed in Appendix A. Candidate dual sensor-actuator degrees of freedom are selected, and minimum acceptable modal active damping factors are specified for the controlled modes. Then the linear programming method uses a linearized analysis to solve for the viscous dashpot constants (same as the gains, but with opposite signs) such that their sum is minimized, all are nonnegative (to

insure stability of all residual modes), and at least the minimum modal active damping factors are produced.

This uncoupled rate feedback technique was evaluated for the same conditions as was coupled rate feedback; namely, joints 1, 2, 4, 5, and 8 were candidates for dual sensor-actuator pairs, and the minimum acceptable modal active damping factor of 0.1 was specified for controlled modes 2-6. The linear programming solution set to zero the feedback gains at joints 1 and 2, leaving active only the dual sensor-actuator pairs at joints 4, 5, and 8. The modal active damping factors actually achieved theoretically are listed in Table 1. Figures 7 and 8 are representative experimental and theoretical frequency response functions for the uncoupled rate feedback. It is evident from these results that this active damping technique was very effective in the application evaluated.

Both coupled and uncoupled rate feedback achieved the objective of actively damping many more modes than there were control actuators. A comparative evaluation of the two techniques would require consideration of additional factors such as control cost, damping of higher residual modes, failure accommodation, etc. At this writing, such an evaluation has not been made.

Figures 5-8 illustrate the general good agreement between experimental measurements and theoretical calculations that has been achieved in this research. Details of the material summarized in this section will be presented in Ref. 8.

2.3 SUBCONTRACT TO HR TEXTRON

HR Textron supported the research at VPI by performing two principal tasks: 1) conduct a review and critical analysis of the VPI control design and experimental setup; 2) apply advanced techniques to design a controller

for actively damping six modes of the VPI pendulous structure using five actuators and existing VPI equipment.

HR Textron's report for the first task is included as Appendix B of this report. Appendix B substantiates previous findings concerning the detrimental effects of bandpass spectral filtering, and it makes several suggestions for improvements. It demonstrates that the modal-space active damping used is a special case of linear quadratic optimal control, and it contends that instability problems arise, at least in part, because state estimation is performed by techniques other than Kalman filtering. The report makes a strong case that Kalman filtering would be helpful.

HR Textron's report for the second task is included as Appendix C of this report. The active damping technique developed in Appendix C is based on the condition that only dual sensor-actuator pairs are used, just as for the VPI coupled rate feedback of Section 3.3. But HR Textron's technique is somewhat more general than VPI's technique inasmuch as explicit requirements are imposed to limit control spillover into and observation spillover from residual modes. HR Textron's technique is proven to be stable. Detailed closed-root roots for HR Textron's technique are given in Appendix C for an example (HR Textron's Case A, with estimator) that is almost directly comparable* with VPI's coupled rate feedback example of Section 3.3. Comparison of the two sets of results shows that the active damping factors achieved by VPI's technique are generally much greater than those achieved by HR Textron's technique. A detailed comparative evaluation of the two techniques has not been made, but a preliminary interpretation is that HR Textron's more general constraints on the control system design actually

---

*The open-loop structure theoretical models were only slightly different in the two examples.

suppress the closed-loop effectiveness. At any rate, it is clear that HR Textron's study was a very useful complement to this research.

3.5 THE PC-1000, A DIGITAL CONTROLLER

All VPI active vibration control experiments conducted before this contract period used analog controllers. These are complicated circuits based on analog electronics; they are tedious and difficult to fabricate, highly susceptible to electrical noise, and difficult to modify. Even an apparently simple change in a control gain (magnitude or sign) can require some circuit teardown and reassembly, which consumes an unreasonable amount of time.

Therefore, an appropriate (capable but inexpensive) digital instrument was sought to replace the analog controllers. Fortunately, such an instrument recently became available. It is the PC-1000 array processor designed and marketed by Systolic Systems Inc. of Campbell, CA. It is essentially a second-generation version of the MCP-100 instrument (Ref. 9) formerly marketed by Integrated Systems Inc. of Palo Alto, CA. The PC-1000 is a small desktop unit, and it is operated from a host IBM-PC personal computer (see Fig. 2). VPI purchased with state money both a PC-1000 and an IBM-PC, the former for $20,000 and the latter for around $3,000.

The PC-1000 is a very effective instrument and is well suited for research in active vibration damping. This was established prior to the purchase in evaluations conducted in the VPI laboratory. Several data acquisition, processing, and control tasks were attempted, including two different strategies for active damping of the VPI beam-cable structure (Refs. 10 and 11). The PC-1000 performed all of the tasks without difficulty and proved to be very flexible and easy to operate, especially in comparison with analog controllers.

The PC-1000 has 16 channels for input signals from sensors, a high

speed array processor for doing calculations with the sensor signals, and 16 channels for output signals to drive control actuators. The sampling rate is adjustable, with the maximum rate being very high indeed: 2000 samples per second. When operated at this high sampling rate with structural vibration frequencies under about 20 Hz, the PC-1000 appears for most practical purposes to be a continuous time (analog) instrument rather than a discrete time (digital) instrument since the phase lag produced by digital data acquisition and processing is very small. The PC-1000 (set at the maximum sampling rate) was used as the controller for all experimental evaluations of coupled and uncoupled rate feedback (see Section 3.3).

The PC-1000's array processor performs one specific operation -- multiplication of a constant 48 x 48 coefficient matrix into a time-varying 48 x 1 vector -- 2000 times per second (if that is the specified sampling rate). Stated mathematically, the operation is

$$\begin{bmatrix} U_{16x1} \\ X1_{32x1} \end{bmatrix} = \begin{bmatrix} F11_{16x16} & F21_{16x32} \\ F12_{32x16} & F22_{32x32} \end{bmatrix} \begin{bmatrix} Y_{16x1} \\ X0_{32x1} \end{bmatrix}$$

Y is the vector of input signals received from sensors, U is the vector of output signals sent to actuators, X0 is a vector of "current" internal state variables, and X1 is a vector of "updated" internal state variables. The prefix-F submatrices consist of user-specified constants that determine the type of control-estimation-filtering being applied.

The matrix operation above was designed to implement multivariable optimal control with state estimation by Kalman filtering (Ref. 9). However, the form is sufficiently general to accommodate many different types of control-estimation-filtering. For the rate feedback implemented in this

research, only appropriate elements of F11 were nonzero, and all other elements of the 48 x 48 coefficient were nulled.

4. PUBLICATIONS, ACCEPTED AND ANTICIPATED

References 1 and 11 have been accepted and scheduled for publication in early 1985. Reference 7, which is derived in large part from Refs. 4 and 5, is in preparation. Reference 8 is in preparation.

5. PROFESSIONAL PERSONNEL

VPI Personnel:

Principal Investigator: William L. Hallauer Jr.

Graduate Research Assistants:

Russell N. Gehling, M.S. degree received March 1984, M.S. thesis listed as Ref. 5, presently employed by Martin Marietta Denver Aerospace;

Gary R. Skidmore, Ph.D. candidate

George Schamel, M.S. candidate

Dinesh Trivedi, Ph.D. candidate

HR Textron Personnel:

Project Director: Richard Quartararo

Research Engineer: Arun Nayak

6. CONFERENCE PAPERS PRESENTED AND ANTICIPATED

References 1 and 10 were presented and published in conference proceedings in early 1984. An extended abstract proposal for Ref. 8 has been submitted, and the paper is being prepared.

REFERENCES

1. W. L. Hallauer Jr., G. R. Skidmore, and R. N. Gehling, "Modal-Space Active Damping of a Plane Grid Structure: Theory and Experiment," Journal of Guidance, Control, and Dynamics, scheduled for publication in the March-April 1985 edition. Presented at the AIAA Dynamics Specialists Conference, Palm Springs, May 17-18, 1984, AIAA Paper 84-1018, pp. 306-316 in the conference proceedings, AIAA CP845.

2. L. Meirovitch, H. Baruh, R. C. Montgomery, and J. P. Williams, "Nonlinear Natural Control of an Experimental Beam," Journal of Guidance, Control, and Dynamics, Vol. 7(4), July-August 1984, pp. 437-442.

3. J.-N. Aubrun, M. J. Ratner, and M. G. Lyons, "Structural Control for a Circular Plate," Journal of Guidance, Control, and Dynamics, Vol. 7(5), Sept.-Oct. 1984, pp. 535-545.

4. M. A. Masse, "A Plane Grillage Model for Structural Dynamics Experiments: Design, Theoretical Analysis, and Experimental Testing," M.S. Thesis, VPI and SU, 1983.

5. R. N. Gehling, "Experimental and Theoretical Analysis of a Plane Grillage Structure with High Modal Density," M.S. Thesis, VPI and SU, 1984.

6. J. H. Argyris, O. Hilpert, G. A. Malejannakis, and D. W. Scharpf, "On the Geometrical Stiffness of a Beam in Space -- A Consistent V. W. Approach," Computer Methods in Applied Mechanics and Engineering, Vol. 20, 1979, pp. 105-131.

7. W. L. Hallauer Jr., R. N. Gehling, and M. A. Masse, "On the Low Frequency Vibration Modes of a Pendulous Thin-Walled Structure," to be submitted to Experimental Mechanics.

8. G. R. Skidmore and W. L. Hallauer Jr., "Experimental-Theoretical Study of Active Vibration Damping with Dual Sensors and Actuators," proposed for the 1985 AIAA Guidance, Navigation and Control Conference, to be submitted to the Journal of Guidance, Control, and Dynamics.

9. R. H. Travassos, "The MCP-100: A Turnkey System for Implementing Multivariable Flight Control Laws," National Aerospace and Electronics Conference, May 1982.

10. G. R. Skidmore, W. L. Hallauer Jr., and R. N. Gehling, "Experimental-Theoretical Study of Modal-Space Control," 2nd International Modal Analysis Conference, Orlando, Florida, February 6-9, 1984; Proceedings, pp. 66-74.

11. G. R. Skidmore and W. L. Hallauer Jr., "Modal-Space Active Damping of a Beam-Cable Structure: Theory and Experiment," Journal of Sound and Vibration, scheduled for publication in Vol. 100(2), May 1985.

TABLE 1. Theoretically calculated structure-control system roots

Mode	THEORETICAL OPEN-LOOP ROOTS		THEORETICAL CLOSED-LOOP ROOTS			
			COUPLED RATE FEEDBACK		UNCOUPLED RATE FEEDBACK	
	Freq. (Hz)	Damping Factor	Freq. (Hz)	Damping Factor	Freq. (Hz)	Damping Factor
1	0.5809	0.0443	0.6171	0.444	0.7159	0.233
2	0.8699	0.0287	0.8377	0.0977	0.8060	0.549
3	1.349	0.0281	1.336	0.127	1.236	0.184
4	3.190	0.0116	3.213	0.110	3.205	0.117
5	3.488	0.00596	3.570	0.0990	3.539	0.105
6	4.850	0.00651	4.948	0.0885	4.735	0.115
7	5.483	0.00250	5.501	0.00508	5.483	0.00438
8	5.645	0.00215	5.653	0.00303	5.644	0.00335
9	5.952	0.00432	6.505	0.118	5.914	0.0321
10	7.898	0.00325	7.908	0.0273	7.903	0.0186
11	8.182	0.00407	8.468	0.372	8.178	0.0433
12	9.006	0.00405	8.507	0.0470	8.860	0.0328
13	9.457	0.00183	9.159	0.0209	9.422	0.0139
14	11.20	0.002	10.22	0.0403	11.11	0.0313
15	12.87	0.002	12.74	0.0147	12.81	0.0171
16	20.56	0.002	20.56	0.00201	20.56	0.00200
17	24.09	0.002	24.05	0.00648	24.09	0.00371
18	26.37	0.002	26.37	0.00318	26.36	0.00381
19	28.23	0.002	28.23	0.00295	28.23	0.00341
20	29.81	0.002	29.79	0.00453	29.81	0.00270

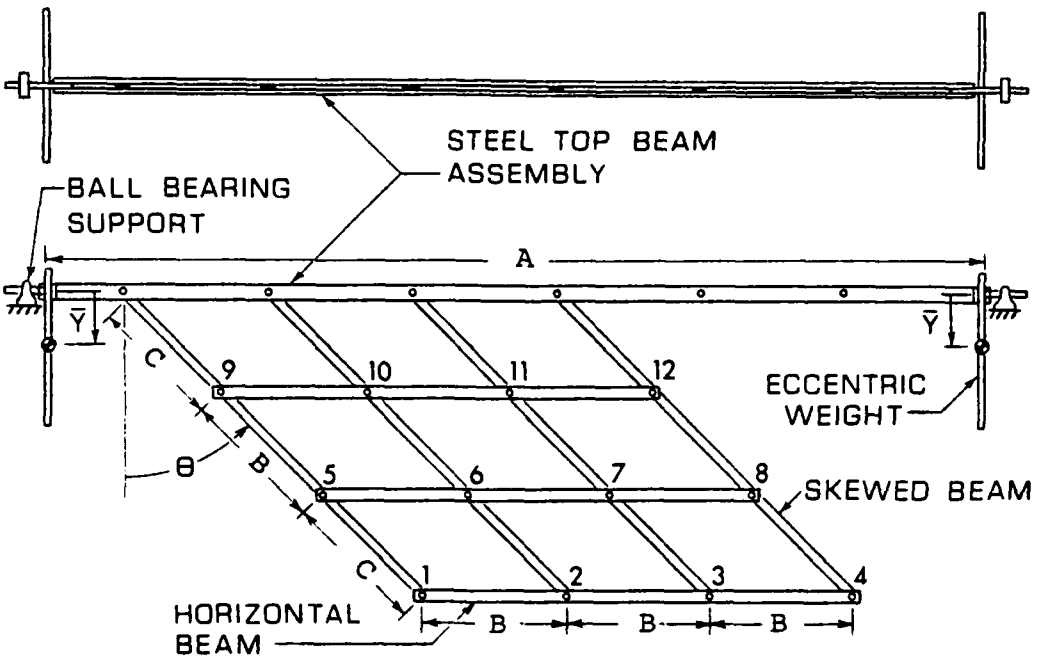

Figure 1. Drawing of the laboratory structure. Geometric parameters: A = 3.96 m; B = 0.610 m; C = 0.591 m; $\bar{Y}$ = 0.216 m; Θ = 46 degrees. Beam cross-section dimensions (in mm): steel beams, 63 x 13; aluminum horizontal beams, 50.8 x 3.2; aluminum skewed beams, 38.1 x 3.2.

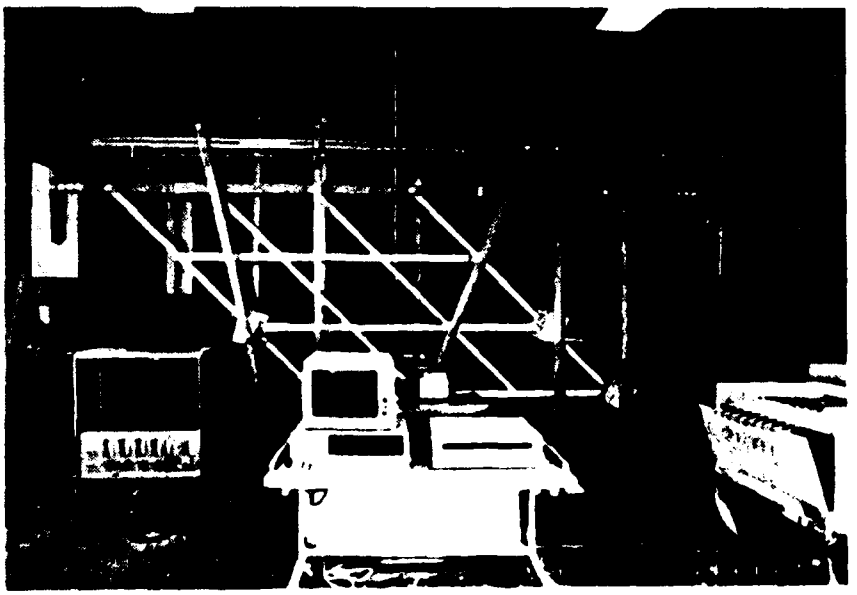

Figure 2. Photograph of laboratory structure. Also shown is the supporting framework for actuators and sensors; PC-1000 controller and host IBM-PC are in the foreground.

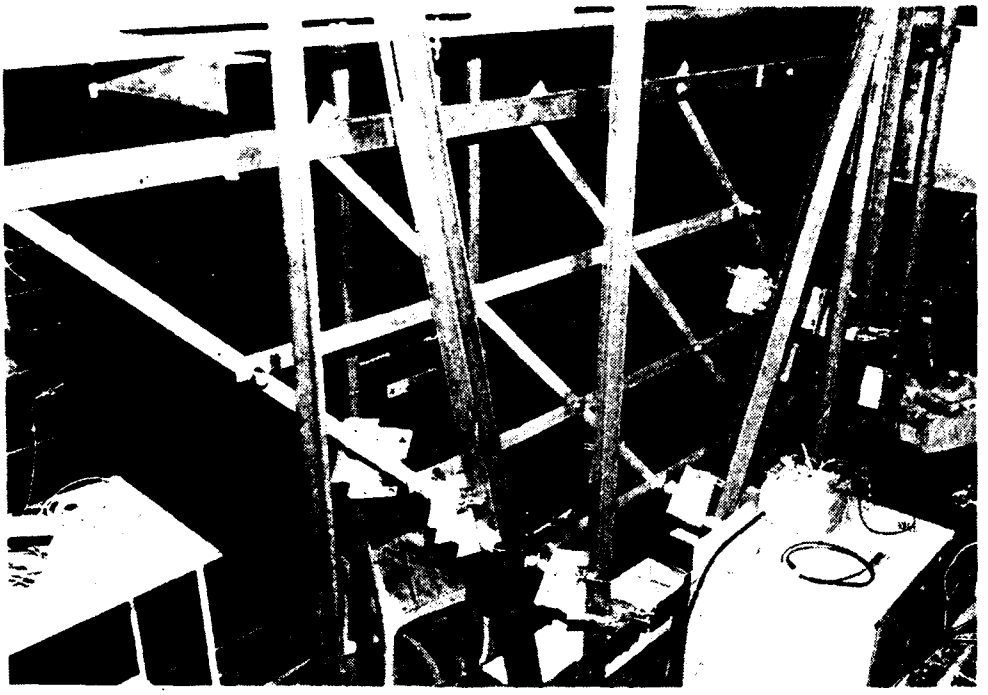

Figure 3. Closeup photograph of laboratory structure. Darker vertical bars are supporting framework.

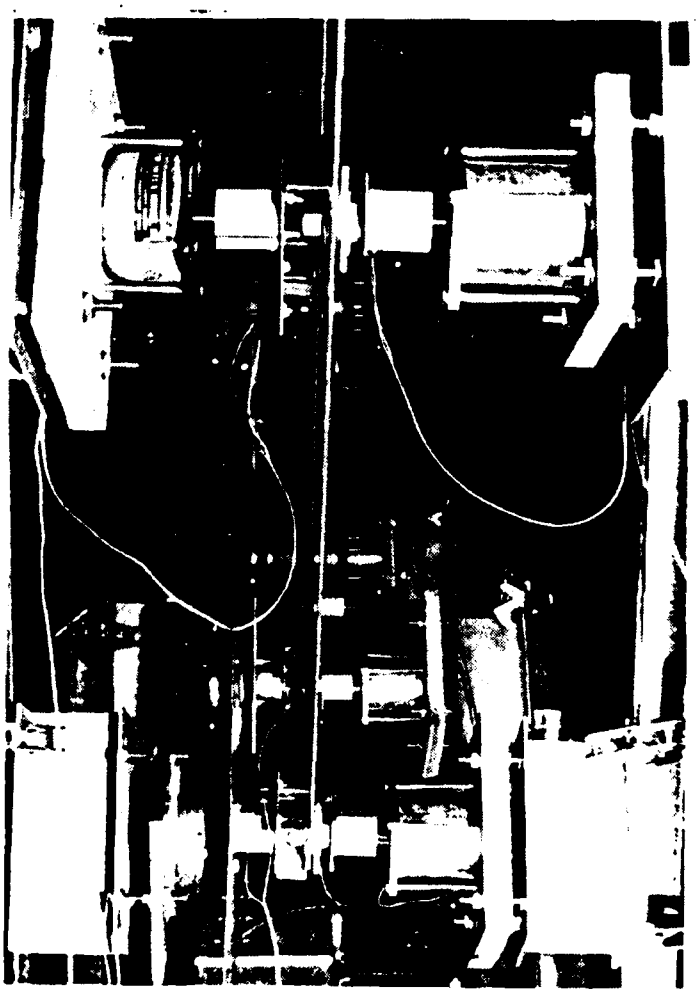

Figure 4. Photograph from the left side of the structure showing several sensor-actuator pairs, with velocity sensors on the right and force actuators on the left.

Photographs on this page by Mark Hill, courtesy of ENGINEERS' FORUM Magazine of VPI & SU

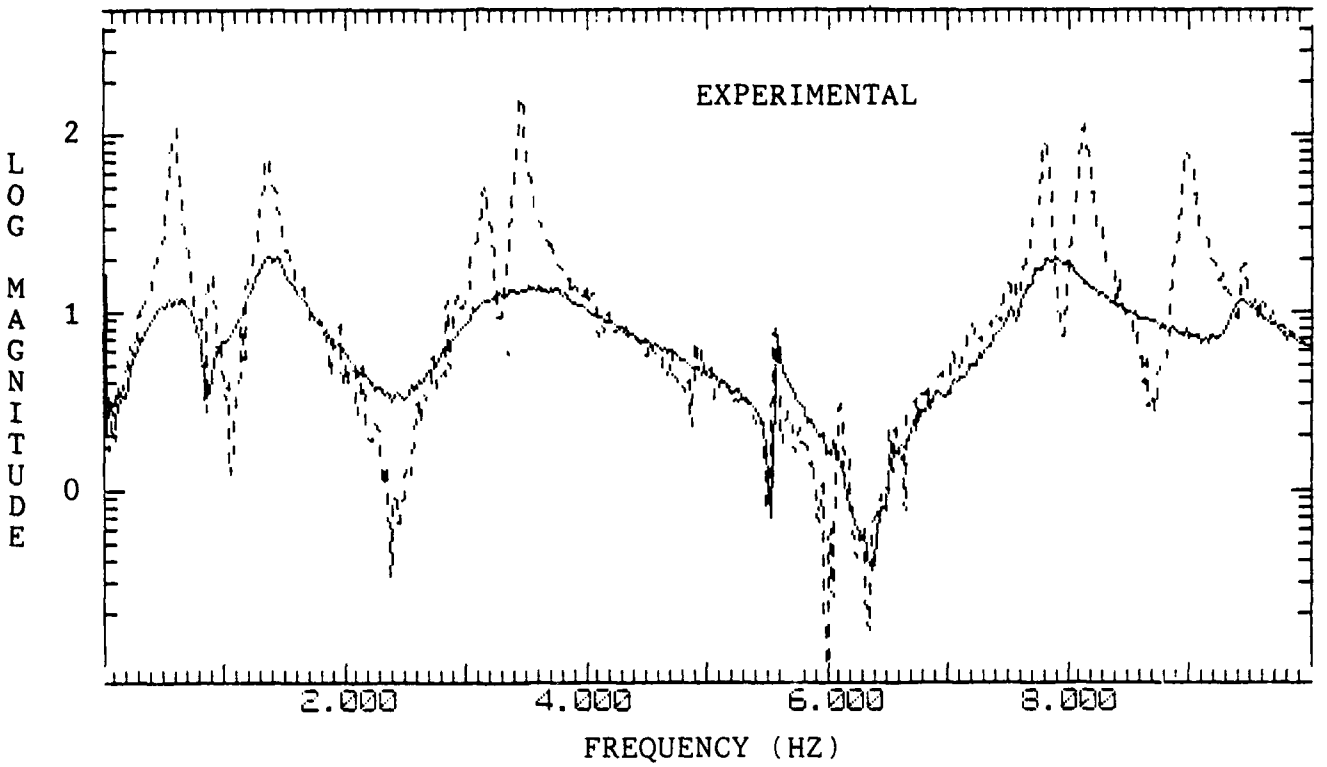

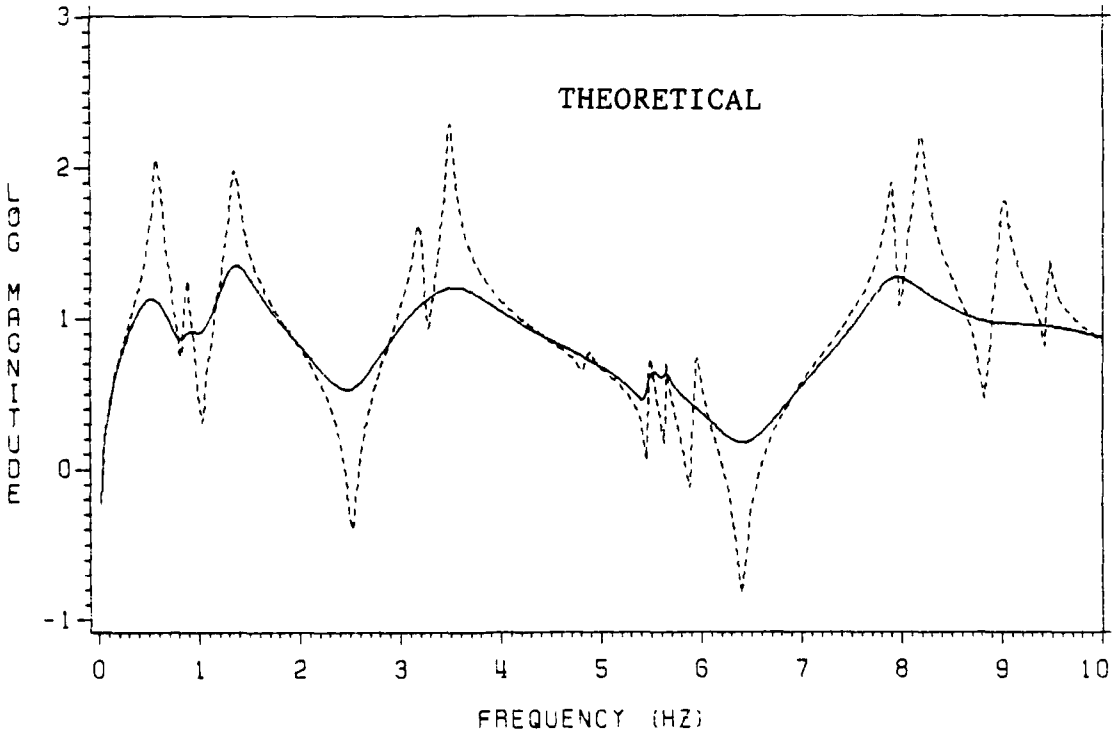

Figures 5. * Velocity frequency response function log magnitude (relative to 5.71E-3 m/s per N)

* Coupled rate feedback (solid curves) and open-loop

* Velocity at joint 2 due to force excitation at joint 2

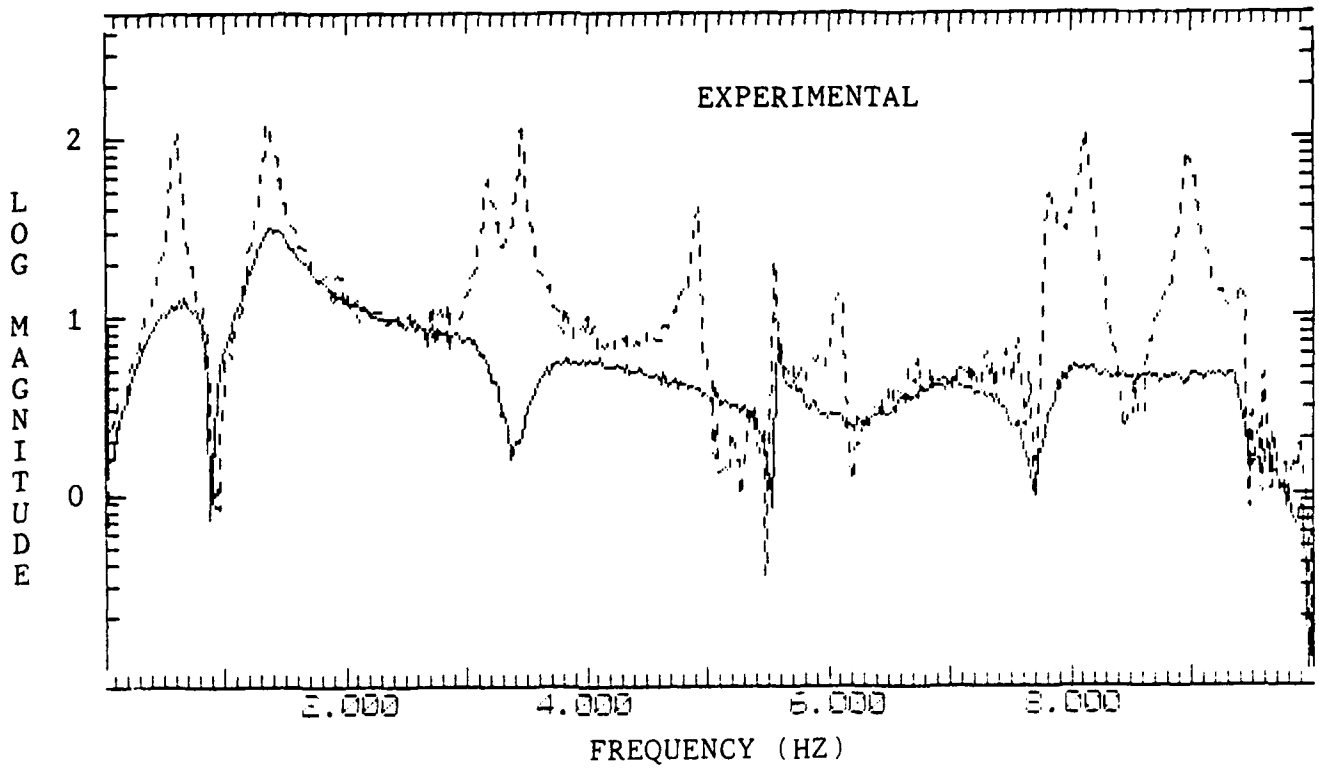

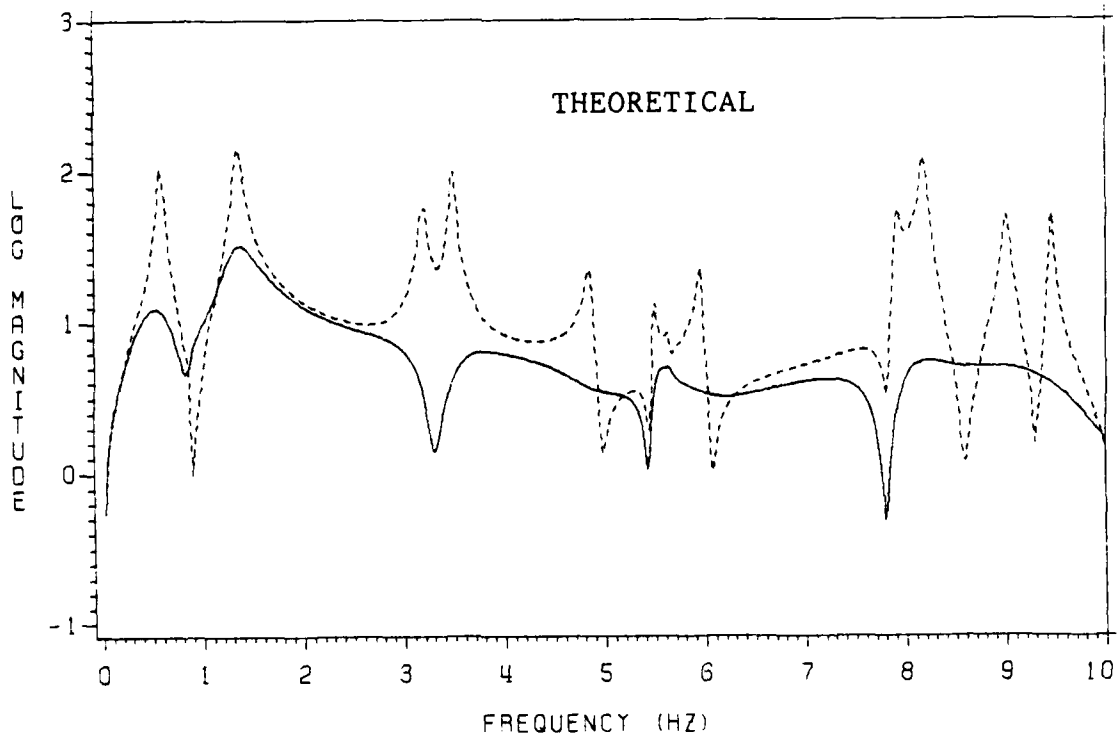

Figures 6. * Velocity frequency response function log magnitude (relative to 5.71E-3 m/s per N)

* Coupled rate feedback (solid curves) and open-loop

* Velocity at joint 1 due to force excitation at joint 2

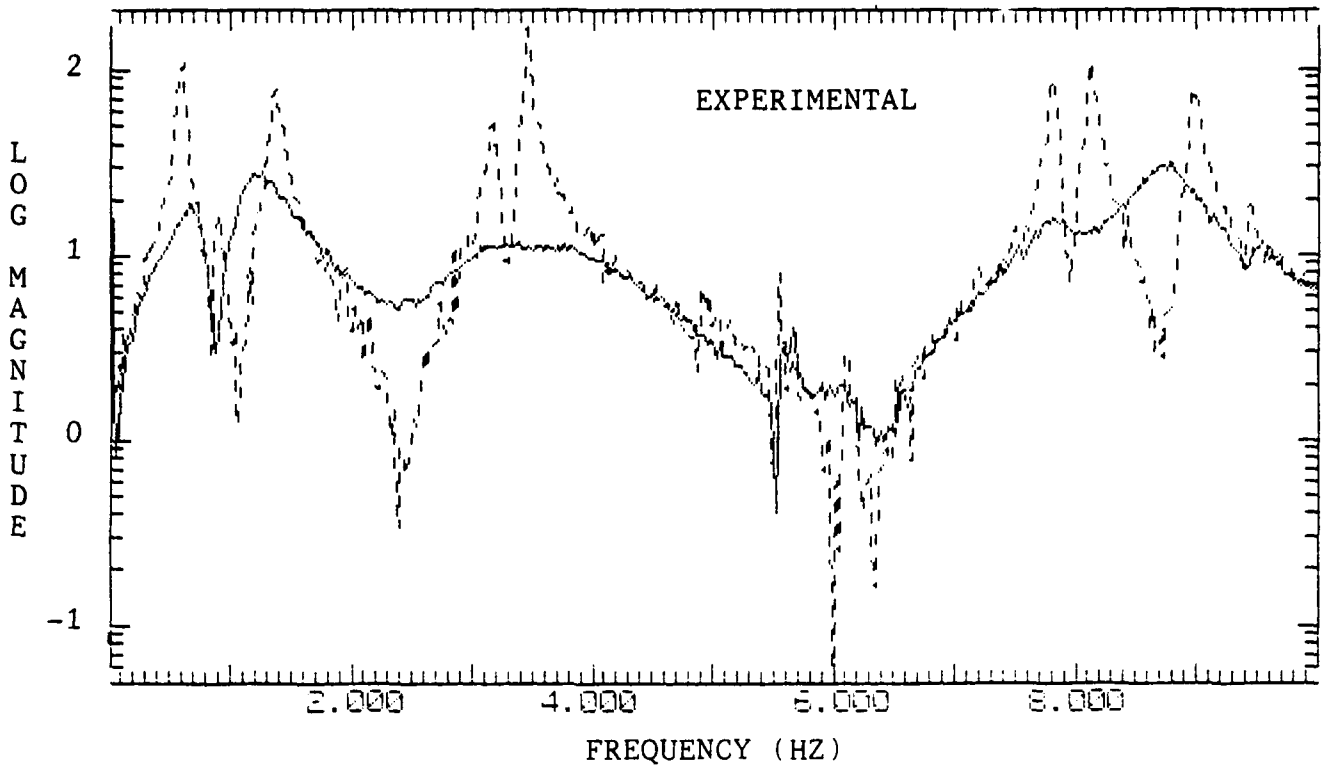

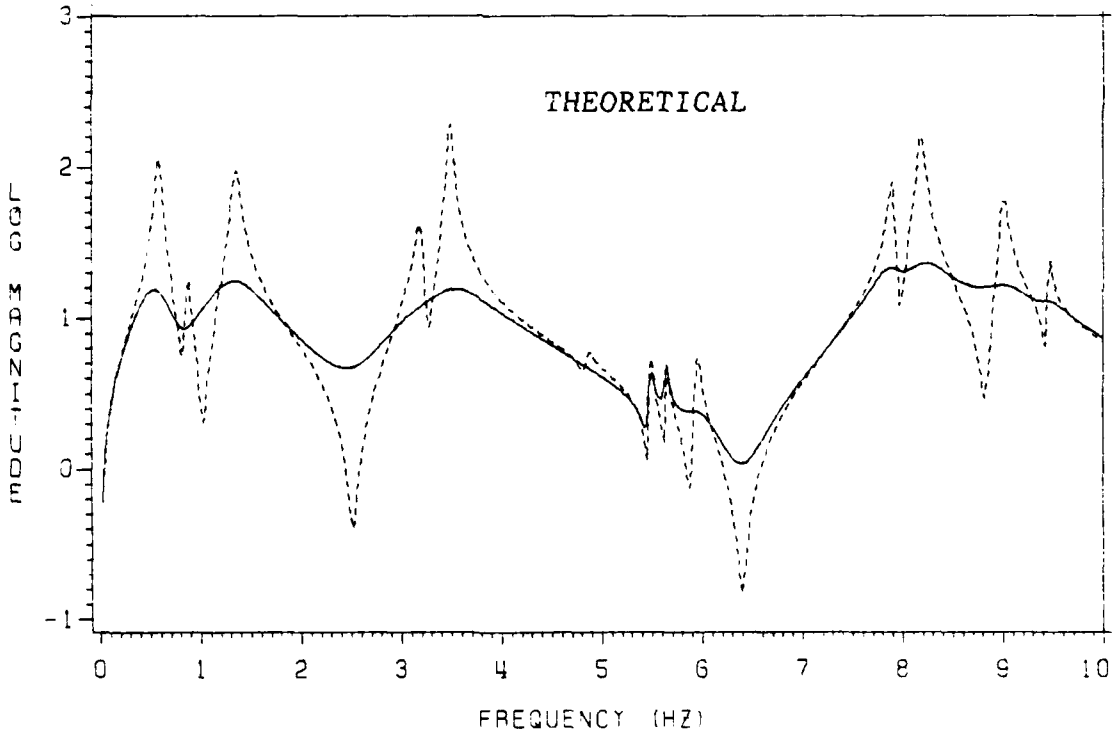

Figures 7. * Velocity frequency response function log magnitude (relative to 5.71E-3 m/s per N)

* Uncoupled rate feedback (solid curves) and open-loop
* Velocity at joint 2 due to force excitation at joint 2

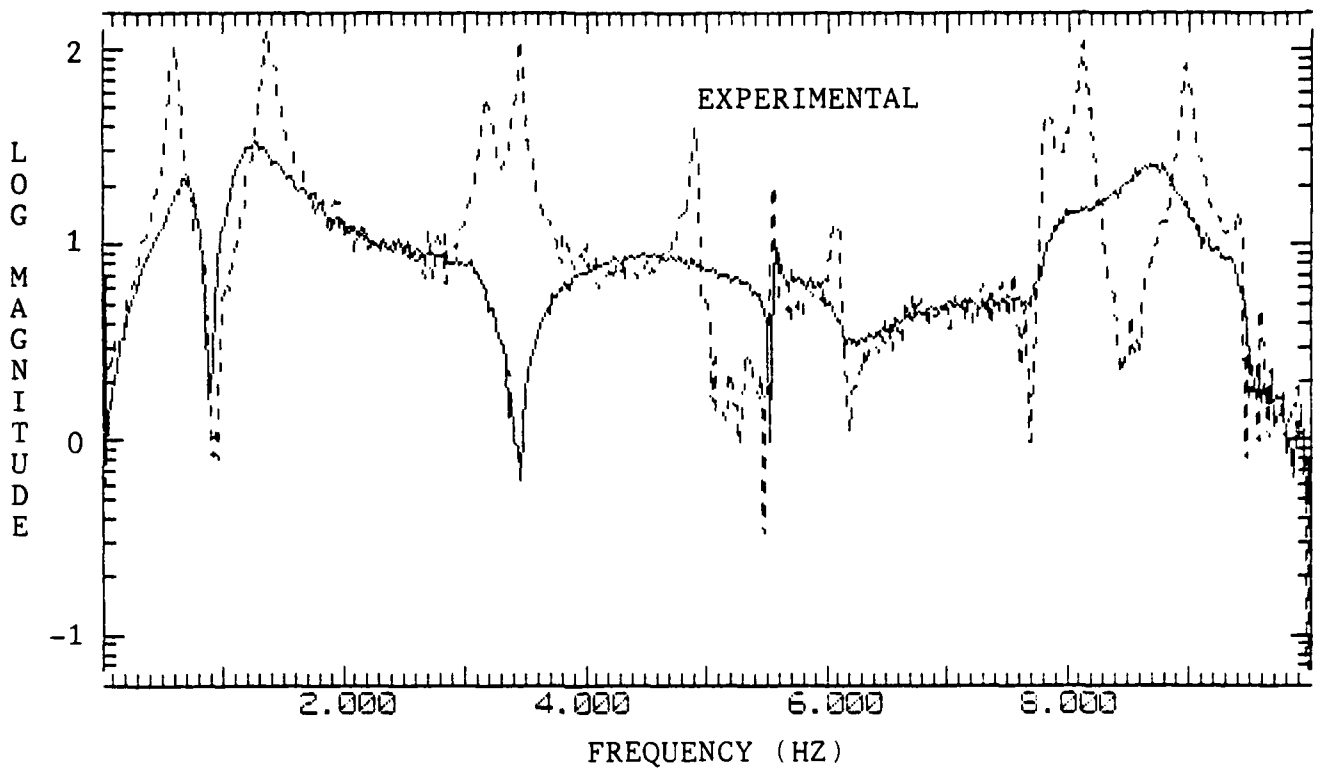

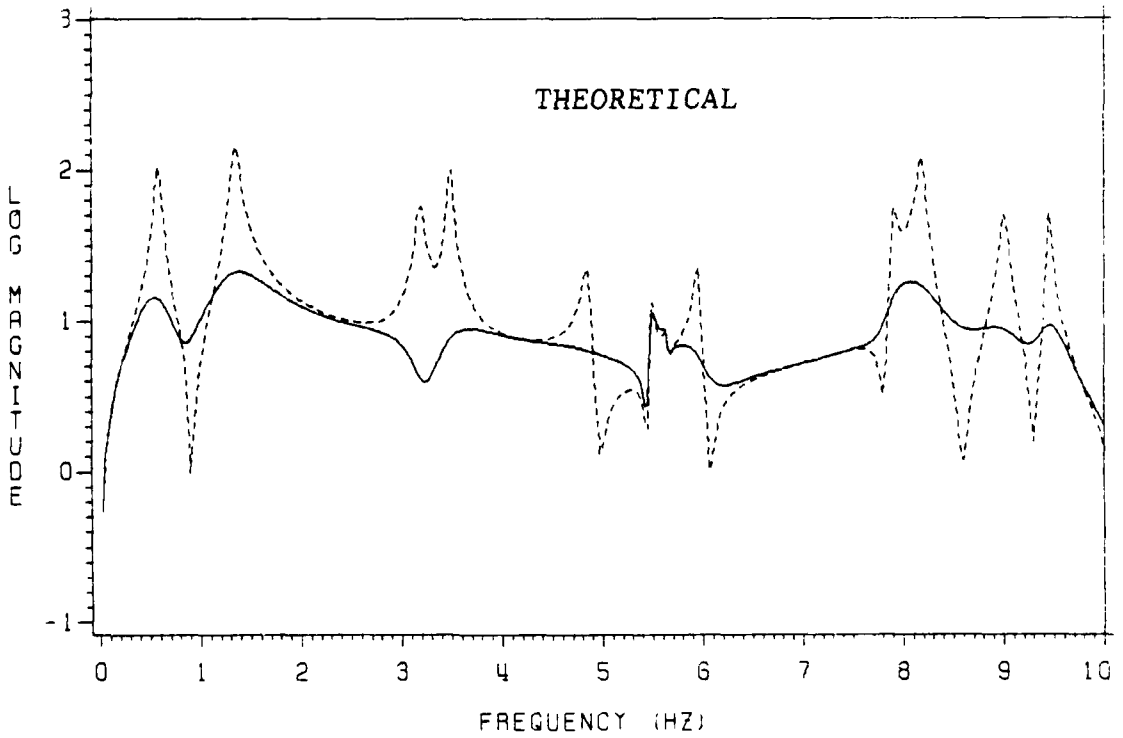

Figures 8. * Velocity frequency response function log magnitude (relative to 5.71E-3 m/s per N)

* Uncoupled rate feedback (solid curves) and open-loop

* Velocity at joint 1 due to force excitation at joint 2

APPENDIX A

THEORETICAL ANALYSIS AND DESIGN OF COUPLED AND UNCOUPLED ACTIVE DAMPING SYSTEMS

A.1 THEORETICAL MODEL

For the purposes of theoretical analysis and control system design, the subject structure is idealized to be linear, with viscous inherent damping that does not couple the normal modes of vibration. It is represented theoretically by an N-degree-of-freedom (DOF) finite element model with the matrix equation of motion in grid point physical displacements $q_i(t)$, $i = 1, 2, \ldots, N$, given by

$$[m]\ddot{\underset{\sim}{q}} + [c]\dot{\underset{\sim}{q}} + [k]\underset{\sim}{q} = \underset{\sim}{e}(t) + \underset{\sim}{f}^c. \tag{1}$$

The N by N matrices [m], [c], and [k] are the mass, noncoupling inherent viscous damping, and stiffness matrices, respectively; $\underset{\sim}{e}(t)$ is the vector of all possible grid point excitations or disturbances; and $\underset{\sim}{f}^c$ is the vector of all grid point control actions.

The truncated modal expansion,

$$\underset{\sim}{q} = \sum_{r=1}^{n_t} \underset{\sim}{\phi}_r \xi_r \equiv [\Phi^t]\underset{\sim}{\xi}^t, \tag{2}$$

transforms the theoretical model from physical to modal coordinates and reduces the order of the model. In Eq.(2), $n_t \leq N$ is the number (truncated) of vibration modes assumed to be active in the response; $\xi_r(t)$, $r = 1, 2, \ldots, n_t$, are the modal coordinates; and $\underset{\sim}{\phi}_r$ are the mode shape vectors. Substituting Eq.(2) into Eq.(1) and applying standard orthogonality conditions gives the modal equations of motion,

$$[M^t]\ddot{\underset{\sim}{\xi}}^t + [C^t]\dot{\underset{\sim}{\xi}}^t + [K^t]\underset{\sim}{\xi}^t = [\Phi^t]^T(\underset{\sim}{e} + \underset{\sim}{f}^c). \quad (3)$$

The modal mass, damping, and stiffness matrices are

$$[M^t] = [\Phi^t]^T[m][\Phi^t] = \text{diag}(M_r,\ r = 1,\ 2,\ \ldots\ ,\ n_t),$$

$$[C^t] = \text{diag}(2M_r\zeta_r\omega_r,\ r = 1,\ 2,\ \ldots\ ,\ n_t),\ \text{and}$$

$$[K^t] = \text{diag}(M_r\omega_r^2,\ r = 1,\ 2,\ \ldots\ ,\ n_t),$$

where ω_r and ζ_r denote, respectively, the natural frequency and inherent viscous damping factor of the r^{th} mode.

The control objective is to specify $\underset{\sim}{f}^c$ in Eqs.(1) and (3) so as to provide stable active damping to the structure. It is presumed that control sensing and actuation are provided by n_d dual sensor-actuator pairs corresponding to a specific subset $\underset{\sim}{q}^d$ of DOF. Accordingly, the n_d by 1 actuator submatrix of $\underset{\sim}{f}^c$ is denoted as $\underset{\sim}{f}^d$, all other elements of $\underset{\sim}{f}^c$ being zero.

It is also necessary to specify a set of n_c controlled, or target, modes that are to be actively damped. All other modes are referred to as residual modes. The control designs are based on the controlled modes, but a by-product of this control is some beneficial active damping in the residual modes. It is assumed in the following that the modal parameters of the controlled modes are known.

Both control designs of interest here depend on rate feedback, so the actuator vector has the fundamental form $\underset{\sim}{f}^d(\dot{\underset{\sim}{q}}^d)$.

A.2 UNCOUPLED RATE FEEDBACK ACTIVE DAMPING

For uncoupled rate feedback, the actuator vector is

$$\underset{\sim}{f}^d = -[UF]\dot{\underset{\sim}{q}}^d,$$

where

$$[UF] = \text{diag}(d_i > 0,\ i \text{ over } n_d).$$

Clearly, [UF] is just a physical viscous active damping matrix associated with the n_d physical DOFs where the dual sensor-actuator pairs are located. This is a physically uncoupled form of feedback for which there exists no communication between non-dual sensors and actuators. It is analogous to the presence of a viscous dashpot at each of the n_d DOFs. Since [UF] is positive definite, this form of active damping can only dissipate energy; it cannot pump energy into the structure. This guarantees the stability of uncoupled rate feedback control, at least for continuous time control which is free of the delays produced by sampling and processing involved in discrete time control.

The uncoupled rate feedback damping constants, d_i, are selected as follows. The desired modal active damping factor in mode s is denoted ζ_s^c. If ζ_s^c is small (less than about 0.3), then one may use the linearized approximation*

$$\sum_i \Phi_{is}^2 d_i = 2M_s \omega_s \zeta_s^c, \qquad (4)$$

to relate modal damping factors to feedback constants. For the special case of $n_c = n_d$ (number of controlled modes equal to the number of sensor-actuator pairs) and with specified values for ζ_s^c, the set of Eqs.(4) for s over n_c can be solved directly for the required d_i values. However, experience with this approach has shown that it usually produces negative values for one or

---

*J.-N. Aubrun, "Theory of the Control of Structures by Low Authority Controllers," Journal of Guidance and Control, Sept.-Oct. 1980, pp. 444-451.

more of the d_i. This is unacceptable, of course, because any d_i < 0 will assuredly produce instability in some residual modes.

Therefore, a linear programming approach for the design of direct rate feedback active damping has been developed which, in a sense, minimizes the control cost while keeping all feedback gains non-negative and somewhat relaxing the constraints on the desired modal active damping factors. One seeks d_i ($i = 1, 2, \ldots, n_d$) such that their sum is minimized, subject to the constraints that all d_i be non-negative and that the resultant modal active damping factors equal or exceed the specified values. In the usual optimization terminology, this is expressed as:

$$\text{minimize} \quad \sum_{i}^{n_d} d_i$$

$$\text{subject to} \quad \sum_{i}^{n_d} \phi_{is}^2 d_i \geq 2M_s\omega_s\zeta_s^c, \; s \text{ over } n_c$$

$$\text{and} \quad d_i \geq 0, \; i \text{ over } n_d.$$

It may be necessary in some applications also to place an upper bound on $\Sigma\, \phi_{is}^2 d_i$ in order to keep the modal damping factors sufficiently low that Eq.(4) remains reasonably accurate. This was not found to be necessary in the present application. Because Eq. (4) is approximate, use of the design method described above generally produces actual closed-loop modal active damping factors somewhat different than those predicted by the linear programming solution. In our application, the actual results have been satisfactorily close to or greater than the predictions.

A.3 COUPLED RATE FEEDBACK ACTIVE DAMPING

The second control design considered here is based on modal-space active damping. Using Eqs.(3) and the actuation vector $\underset{\sim}{f}^d$, with the disturbance vector $\underset{\sim}{e}$ omitted, one writes the modal equations for the controlled modes alone as

$$[M^c]\ddot{\underset{\sim}{\xi}}^c + [C^c]\dot{\underset{\sim}{\xi}}^c + [K^c]\underset{\sim}{\xi}^c = [\Phi^{dc}]^T\underset{\sim}{f}^d. \tag{5}$$

Superscript c in Eq.(5) denotes appropriate partitions of the matrices in Eq.(3). In particular, the partition of $[\Phi^t]$ with n_d rows corresponding to the sensed DOFs ($\underset{\sim}{q}^d$) and n_c columns corresponding to the controlled modes ($\underset{\sim}{\xi}^c$) is denoted $[\Phi^{dc}]$. For this application of modal-space active damping, we restrict the number of controlled modes to equal the number of sensor-actuator pairs ($n_c = n_d$), so that $[\Phi^{dc}]$ is square; moreover, the parameters must be chosen so that this matrix is nonsingular. It is clear from Eq.(5) that one can, in principle, produce specified modal viscous active damping in each controlled mode by defining the control actuation to be

$$\underset{\sim}{f}^d = -[\Phi^{dc}]^{-T}[D^c]\dot{\underset{\sim}{\xi}}^c, \tag{6}$$

where

$$[D^c] = \text{diag}(2M_s\omega_s\zeta_s^c,\ s \text{ over } n_c).$$

But $\dot{\underset{\sim}{\xi}}^c$ in Eq. (6) cannot be inferred exactly, either by direct measurement or, evidently, by any form of filtering. Hence, we define next a simple but effective estimate, $\hat{\dot{\underset{\sim}{\xi}}}^c$. From the modal expansion, Eq.(2), the measured physical velocities are written as

$$\dot{\underset{\sim}{q}}^d = [\Phi^{dt}]\dot{\underset{\sim}{\xi}}^t = [\Phi^{dc}]\dot{\underset{\sim}{\xi}}^c + [\Phi^{dr}]\dot{\underset{\sim}{\xi}}^r, \tag{7}$$

where superscript r denotes residual modes. Equation (7) shows

that, for relatively small residual mode response, a reasonable estimate for controlled mode response is

$$\hat{\dot{\underset{\sim}{\xi}}}^c = [\Phi^{dc}]^{-1}\dot{\underset{\sim}{q}}^d. \tag{8}$$

It cannot, of course, be guaranteed that the response of the residual modes will be small. Nevertheless, Eq.(8) is a good choice for an estimate because it contributes greatly to the stability of the structure-control system, as will be shown next. The estimate given by Eq.(8) and other versions of this concept have been used previously, appearing under the names static observation (Ref. 3 of the report) and modal filtering (Ref. 2 of the report).

Using Eq.(8) for $\dot{\underset{\sim}{\xi}}^c$ in Eq.(6) gives

$$\underset{\sim}{f}^d = -[CF]\dot{\underset{\sim}{q}}^d,$$

where the physical, coupled feedback matrix is given by

$$[CF] = [\Phi^{dc}]^{-T}[D^c][\Phi^{dc}]^{-1}. \tag{9}$$

Viscous active damping matrix [CF] is a nondiagonal, symmetric matrix which contains coupling terms between all sensors and actuators. Most importantly, [CF] is always positive definite; this is evident from the quadratic form of Eq.(9) with a positive definite, diagonal modal active damping matrix $[D^c]$. Therefore, this coupled rate feedback form of modal-space active damping, which has every sensor dual with an actuator, can only increase the damping in all modes, residual as well as controlled, and is guaranteed to produce a stable structure-control system. Another physical interpretation of this active damping technique is that it produces only beneficial spillover in the residual modes.

Equation (9) demonstrates also that this technique is

stability-robust relative to errors in the modal parameters. [CF] is positive definite regardless of the accuracy of $[\phi^{dc}]$ and of the modal parameters in $[D^c]$.

It might be expected that using more sensors than actuators would improve the accuracy of $\hat{\dot{\underset{\sim}{\xi}}}^c$ and therefore would improve active damping performance. We have tested this hypothesis theoretically and have found that modal response accuracy is indeed improved. However, active damping performance is inevitably seriously compromised in the sense that some residual modes become unstable. In this case, the spillover into these residual modes is detrimental. This type of instability occurs whenever the control sensors are not completely dual with the control actuators. For such a case, the physical viscous active damping matrix is, in general, not positive definite.

Because Eq. (8) is only an estimate for $\dot{\underset{\sim}{\xi}}^c$, the actual closed-loop modal active damping factors achieved by this coupled rate feedback method generally are somewhat different from those specified in Eq. (6). In our application, the actual values achieved have been satisfactorily close to or greater than the specified values.

A.4 THEORETICAL ANALYSIS OF THE STRUCTURE-CONTROL SYSTEM

The quantitative theoretical analysis of system dynamic characteristics consists of calculation of eigenvalues (system roots) and frequency response functions (FRF). Equation (3) is rearranged as

$$[M^t]\ddot{\underset{\sim}{\xi}}^t + [C^t]\dot{\underset{\sim}{\xi}}^t - [\phi^{dt}]^T\underset{\sim}{f}^d + [K^t]\underset{\sim}{\xi}^t = [\phi^t]^T\underset{\sim}{e} \qquad (10)$$

where $\underset{\sim}{f}^d$ can take on either of the previously derived forms for

the closed-loop systems, or can be set equal to zero for the open-loop case. In general, $\underset{\sim}{f}^d$ has the form

$$\underset{\sim}{f}^d = -[F]\dot{\underset{\sim}{q}}^d$$

where [F] is a matrix of physical feedback gains (either [UF] or [CF]). In terms of the modal response, truncated to n_t modes, this becomes

$$\underset{\sim}{f}^d = -[F][\Phi^{dt}]\dot{\underset{\sim}{\xi}}^t$$

which is substituted into Eq.(10) to give

$$[M^t]\ddot{\underset{\sim}{\xi}}^t + ([C^t] + [\Phi^{dt}]^T[F][\Phi^{dt}])\dot{\underset{\sim}{\xi}}^t + [K^t]\underset{\sim}{\xi}^t = [\Phi^t]^T\underset{\sim}{e}. \qquad (11)$$

For calculation of system eigenvalues, Eq.(11) is written in its homogeneous form

$$[M^t]\ddot{\underset{\sim}{\xi}}^t + [AD]\dot{\underset{\sim}{\xi}}^t + [K^t]\underset{\sim}{\xi}^t = \underset{\sim}{0} \qquad (12)$$

with $[AD] = ([C^t] + [\Phi^{dt}]^T[F][\Phi^{dt}])$ representing the total damping matrix. A state vector is defined as

$$\underset{\sim}{x} = \begin{bmatrix} \dot{\underset{\sim}{\xi}}^t \\ \underset{\sim}{\xi}^t \end{bmatrix}$$

to facilitate the formulation of an equivalent set of $2n_t$ first-order differential equations,

$$\begin{bmatrix} [0] & [M^t] \\ [M^t] & [AD] \end{bmatrix} \begin{bmatrix} \ddot{\underset{\sim}{\xi}}^t \\ \dot{\underset{\sim}{\xi}}^t \end{bmatrix} - \begin{bmatrix} [M^t] & [0] \\ [0] & -[K^t] \end{bmatrix} \begin{bmatrix} \dot{\underset{\sim}{\xi}}^t \\ \underset{\sim}{\xi}^t \end{bmatrix} = \begin{bmatrix} \underset{\sim}{0} \\ \underset{\sim}{0} \end{bmatrix}, \qquad (13)$$

which is of the form

$$[B]\dot{\underset{\sim}{x}} - [A]\underset{\sim}{x} = \underset{\sim}{0}.$$

This leads to a standard eigenvalue problem

$$p[B]\underset{\sim}{X} = [A]\underset{\sim}{X},$$

for which the system roots are given by the complex eigenvalues p. For each complex conjugate pair, $p = \sigma \pm i\omega$, one can define a damping factor

$$\zeta = \frac{-\sigma}{\sqrt{\sigma^2 + \omega^2}}$$

and a frequency

$$f = \frac{\sqrt{\sigma^2 + \omega^2}}{2\pi}$$

Frequency response analysis is accomplished with the nonhomogeneous form of Eq.(12),

$$[M^t]\ddot{\underset{\sim}{\xi}}^t + [AD]\dot{\underset{\sim}{\xi}}^t + [K^t]\underset{\sim}{\xi}^t = [\Phi^t]^T\underset{\sim}{e}, \tag{14}$$

where $\underset{\sim}{e}$ usually has only one nonzero term, corresponding to the driving point of the harmonic excitation. For excitation of unit magnitude in DOF k, $e_k = 1$, at frequency ω, Eq. (14) reduces to

$$(-\omega^2[M^t] + i\omega[AD] + [K^t])\underset{\sim}{\Xi}^t = \underset{\sim}{E}_k \tag{15}$$

where $\underset{\sim}{E}_k$ is the k^{th} column of $[\Phi^t]^T$ and $\underset{\sim}{\Xi}^t$ represents the vector of frequency responses in the modal coordinates. This n_t-vector is calculated for any specified value of ω by direct solution of Eq. (15). The complex displacement frequency response in DOF j due to forcing in DOF k is obtained from modal expansion Eq. (2),

$$DFRF_{j,k}(\omega) = \Sigma\ \Phi^t_{jr}\Xi^t_r(\omega).$$

Finally, the velocity frequency response function is

$$VFRF_{j,k}(\omega) = i\omega DFRF_{j,k}(\omega).$$

APPENDIX B

ANALYSIS OF THE

VPI ACTIVE STRUCTURAL DAMPING EXPERIMENT

JULY 18, 1984

ARUN P. NAYAK, PhD

HR TEXTRON INC.
SYSTEMS ENGINEERING DIVISION
2485 McCabe Way
IRVINE, CALIFORNIA 92714
(714) 660-0253

INTRODUCTION AND SUMMARY

This report analyzes the control system for the VPI active vibration suppression experiment.

The test article consists of a grid-like structure that hangs from a pivoted overhead support bar. Five voice coil actuators apply control forces to the structure, and one velocity sensor provides measurements for the control system. The control concept is based on independent control of each mode, with the actuators applying forces proportional to modal velocity in order to actively damp structural oscillations. The reader is referred to Hallauer, et al, Reference (1) for a more detailed description of the test configuration.

The following sections review the control concept, analyze the test article control system, interpret the analytical results and present recommendations for improving performance. The analysis of the existing test setup shows that there is an instability at 3.27 Hz that apparently is caused by a structural dynamic/sensor filter interaction. This result verifies similar analytical and experimental results obtained by Hallauer, et al, Reference (1).

A discussion and further analysis of the instability indicate that the test article control system uses a Linear Quadratic Regulator controller. However, since the

filter is not a Kalman filter, the principle of separation of controller and filter does not apply. Therefore, there is, in general, no a priori guarantee that the combined controller and filter will be stable, as there would be with a Kalman filter and Linear Quadratic Regulator controller.

Suggestions for improving control system performance are provided. Significant performance improvements could be obtained by using a Kalman filter to construct modal velocity estimates from the one velocity sensor. An alternate approach is to use 6 velocity sensors and a spatial filter to algebraically transform the velocity response at 6 nodes into 6 modal velocities. Spillover effects could be avoided by using a low-pass temporal filter and locating the sensors near zero displacements of the lowest frequency uncontrolled modes.

A third approach, which involves minimal changes to the existing test setup, is analyzed. It uses the existing narrow band temporal filters and velocity sensor to measure the modal velocities of the first three controlled modes. The other two modal velocities are measured by passing the signals from the existing velocity sensor and a new velocity sensor at node 13 through temporal filters each having a bandwidth that includes the natural frequencies of both modes. The resulting signals are then passed through a 2 x 2 spatial filter to algebraically transform to modal

velocities. An analysis of this approach shows that it is stable; however, the desired active damping values are not achieved.

It is apparent that the unstable behavior of the existing test article and the less than desired performance of the third suggested modification is due to the dynamics of the narrow band temporal filters.

CONTROL CONCEPT REVIEW

The theory is briefly reviewed here. For more details refer to the paper by Hallauer, et al, Reference (1).

The equations of the evaluation model can be written as:

$$\ddot{\underline{\xi}} + [C]\dot{\underline{\xi}} + [K]\underline{\xi} = [\phi^a]^T \underline{C}^a \qquad (1)$$

where

$\underline{\xi}(t)$ = Nx1 vector of modal coordinates

$[C]$ = diag $(2\zeta_r\omega_r,\ r = 1, .., N)$

$[K]$ = diag $(\omega_r^2, r = 1, .., N)$

ζ_r and ω_r = the natural frequency and inherent viscous damping factor of the rth mode

$\underline{C}^a$ = the 5x1 vector of the actuator forces

$[\phi^a]^T$ = the control matrix, which is a submatrix of the modal matrix $[\Phi]$

N = 10, the number of modes considered for the evaluation model.

Feedback control $\underline{C}^a$ is assumed to be a function of only velocity, in accordance with the VPI test article.

$$\underline{C}^a = [C^{ac}]\ [\phi_i^c]\dot{\underline{\xi}}^c \tag{2}$$

$[C^{ac}]$ is a control apportioning matrix that is to be selected later. $[\phi_i^c]$ is a submatrix of the modal matrix $[\phi]$. $\dot{\underline{\xi}}^c$ is the velocity of the modes to be controlled. The present study is concerned with controlling 5 modes, modes 2 through 6. The control, as suggested by Equation (2), will add active damping in modes 2 through 6.

$$\dot{q}_i^c = [\phi_i^c]\dot{\underline{\xi}}^c \tag{3}$$

is the output of the ideal spectral filter corresponding to the particular modal velocity $\dot{\underline{\xi}}^c$. The input to this ideal filter is $\dot{q}_i$, the velocity of the ith node.

The control apportioning matrix is chosen in the following way.

$$[C^{ac}] = -[\phi^{ac}]^T\ [D^c]\ [\phi_i^c]^{-1} \tag{4}$$

$[\phi^{ac}]^T$ is an appropriate submatrix of $[\phi^c]$, corresponding to the modes to be controlled. $[D^c]$ = diag ($2\zeta_s^c\omega_s$, s varies over the controlled modes). ζ^c is the viscous active damping factor specified for mode s, and for the purposes of the stability analysis ζ_s^c is taken to be 0.1 for all modes to be controlled.

Since an ideal filter is impossible to make, the output

of a real filter is used for the feedback purposes. Let $\underline{y}$ be the output of the real spectral filter, then the control $\underline{c}^a$ will be given by

$$\underline{c}^a = [c^{ac}]\underline{y} \tag{5}$$

The real spectral filter is modelled as

$$\ddot{\underline{y}} + [B]\ \dot{\underline{y}} + [\omega_f^2]\underline{y} = [B]\ [1]\ddot{q}_1 \tag{6}$$

[1] is a vector of ones. $\dot{q}_1$ is the measured velocity of node 1; the VPI test setup can measure only this velocity at present. [B] is the diagonal matrix of filter half-power bandwidths and $[\omega_f^2]$ is the diagonal matrix of the filter center frequencies squared.

STABILITY ANALYSIS OF THE TEST ARTICLE

The new 56 DOF model data supplied by VPI, Reference (2), was used for the purposes of the stability analysis. The ten lowest frequency modes were used in the evaluation model.

The stability analysis results coincide fairly well with those presented by Hallauer, et al, Reference (1). The results, which are summarized in Table 1, contain the damping ratios and frequencies of structural and filter modes for open- and closed-loop systems. Four different closed-loop cases are treated. In the first closed-loop case, the bandwidth of the filter is reduced to 1/10th the original bandwidth. This case is stable. Hallauer, et al, Reference (1)

TABLE 1

ONE SENSOR SYSTEM

MODE TYPE*	OPEN LOOP		CLOSED LOOP							
			CASE 1		CASE 2		CASE 3		CASE 4	
	ζ_r	f_r	ζ_r	f_r	ζ_r	f_r	ζ_r	f_r	ζ_r	f_r
SM1	.043	.584	.0427	.4535	.1226	.2546	.1406	.2336	.1405	.2335
SM2	.05	.89	.0499	.8789	.051	.8787	.0511	.87	.0511	.8787
FM2	.5618	.78	.0611	1.1927	.3264	1.349	.3932	1.352	.3932	1.3519
SM3	.035	1.37	.0228	1.2404	.014	1.323	.0198	1.32	.020	1.3267
FM3	.3642	1.37	.0361	1.4831	.1964	2.284	.2504	2.5016	.2334	2.4746
SM4	.01	3.27	.0075	3.20	.0069	2.952	-.0133	2.9028	.0023	2.9554
FM4	.0503	3.27	.0076	3.36	-.0142	3.432	-.0136	3.4321	.038	3.6097
SM5	.009	3.593	.0066	3.507	.0632	3.4283	.0727	3.4264	.009	3.593
FM5	.0459	3.593	.0069	3.67	.0226	3.8813	.0266	3.9523	.049	3.593
SM6	.013	4.957	.0115	4.797	.0469	4.462	.0575	4.3738	.0524	4.3769
FM6	.1009	4.947	.0115	5.1146	.041	5.4034	.0493	5.4621	.0533	5.4913
SM7	.0035	5.485	.003	5.486	.006	5.49	.0063	5.4864	.0045	5.4791
SM8	.0030	5.654	.003	5.654	.003	5.654	.0030	5.654	.003	5.654
SM9	.0060	6.194	.006	6.194	.0069	6.194	.0076	6.194	.0053	6.12
SM10	.0060	7.997	.006	7.998	.0061	8.0093	.0062	8.0216	.006	7.99

*SM_r - Denotes Structure Mode r

FM_r - Denotes Filter Mode r

Case 1: - Filter bandwidth is 1/10 of the test article bandwidth

Case 2: - Filter bandwidth is 8/10 of the test article bandwidth

Case 3: - Test article bandwidth

Case 4: - Controlling only 4 modes; system modes 2, 3, 4 and 6

obtained similar results. In the second closed-loop case, the bandwidth of the filter is 8/10th of the original bandwidth. For this case filter mode 4 shows instability. Case 3 is the closed-loop system used in the test article; it has two unstable modes. A review of the eigenvectors corresponding to these two modes shows strong interaction between filter mode 4 and system mode 4. Thus, one may conclude that these modes might be driving each other to instability. There is a slight discrepancy here with the numerical results of Hallauer, et al, Reference (1), probably because different data sets were used; however, the overall conclusions are the same. The fourth closed-loop case deals with controlling only 4 modes, and this system is stable. This result coincides with those of Hallauer, et al, Reference (1).

DISCUSSION OF STABILITY RESULTS

The controller and the filter are usually synthesized on the premise that they can be separately designed and, when they are put together to form a compensator, they will be stable and perform as expected from the separate analyses. This method, sometimes called the principle of separation of controller and filter, does not always work. The results obtained here show that the principle cannot be applied to obtain an optimal compensator in this case.

The principle of separation of controller and estimator can be applied to obtain an optimal compensator if the problem can be posed as a Linear Quadratic Gaussian (LQG) problem. The LQG controller is a solution to the Linear Quadratic Regulator (LQR) problem, and the filter is a Kalman filter.

The test article controller was devised in an intuitive way; however, the analysis below shows that it is also a solution to the LQR problem. But, since the filter is not a Kalman filter, there is no guarantee that the separation of controller and filter yields an optimal control. In fact, the stability analysis results suggest that the test article compensator is not at all close to optimal. Hence, it is recommended that the filter be improved.

OPTIMAL VELOCITY FEEDBACK CONTROL USING THE LQR SOLUTION

Consider the following

$$\ddot{\underline{\xi}}^c + [C^c]\dot{\underline{\xi}}^c + [K^c]\underline{\xi} = [\phi^{ac}]^T \underline{C}^a \qquad (7)$$

$[C^c]$ and $[K^c]$ are proper submatrices of the [C] and [K] matrices corresponding to $\underline{\xi}^c$, the modes to be controlled.

The optimality criterion is

$$J = \int_0^\infty \left([\underline{\xi}^{c^T} \dot{\underline{\xi}}^{c^T}] \begin{bmatrix} Q_1 & 0 \\ 0 & Q_3 \end{bmatrix} \begin{bmatrix} \underline{\xi}^c \\ \dot{\underline{\xi}}^c \end{bmatrix} + \underline{C}^{a^T} [R]\, \underline{C}^a \right) dt \qquad (8)$$

where $[Q_1]$ and $[Q_3]$ are positive semi-definite weighting

matrices for $\underline{C}^a$.

The optimal control in general is given by

$$\underline{C}^a = -[K_1]\underline{\xi}^c - [K_2]\dot{\underline{\xi}}^c \qquad (9)$$

But by judicious choice of $[Q_1]$, $[Q_3]$ and $[R]$ one can obtain $[K_1] = 0$. Thus

$$\underline{C}^a = -[K_2]\dot{\underline{\xi}}^c \qquad (10)$$

is the desired optimal velocity feedback control. By some trial and error, the values

$$[Q_1] = 0$$

$$[Q_3] = \text{diag } (2.5, 5.0, 20.0, 24.0, 49.0)$$

$$[R] = [\phi^{ac}]\ [\phi^{ac}]^T$$

were found to yield almost identical results as those of the test article controller.

Thus, if a Kalman filter is implemented instead of the current filter, optimal control will be achieved.

RECOMMENDATIONS TO IMPROVE PERFORMANCE

In the present context, in order to improve the stability of the VPI test article without changing much of the existing facilities, the placement of a second velocity sensor is suggested. An analysis given below does indeed show that a second sensor improves the stability of the system.

It is thought that it will be convenient to put the

second sensor colocated with some other actuator as was done with the first sensor. Thus, the second sensor can be colocated with any one of the other four actuators. The analysis presented herein finds a proper colocated position for the second sensor.

Earlier it was shown that the controller by itself is optimal, hence the apportioning matrix $[C^{ac}]$ is not changed, but a new filter output is obtained by using these two sensor outputs.

Since the instability is believed to be caused by two closely placed modes, it is attempted to separate them using two sensor outputs and a modified filter as illustrated on the following page. $\underline{y}_1$ and $\underline{y}_i$ are the new filter outputs corresponding to the measured velocities at node 1 and node i. $y_{1,4}$ and $y_{i,1}$ are the components of $\underline{y}_1$ and $\underline{y}_i$ and they are related to mode 4 and mode 5 as follows:

$$y_{1,4} = \alpha[\phi_{1,4} \quad \phi_{1,5}] \begin{bmatrix} \dot{\xi}_4 \\ \dot{\xi}_5 \end{bmatrix} \tag{11}$$

$$y_{i,1} = \alpha[\phi_{i,4} \quad \phi_{i,5}] \begin{bmatrix} \dot{\xi}_4 \\ \dot{\xi}_5 \end{bmatrix} \tag{12}$$

α reflects the fact that the center frequency of the above filter is not the frequency of the modes but is the average of the square of the center frequency of mode 4 and mode 5. But considering the proximity of the frequencies and broad half-power bandwidth, which is 1, the value of α is assumed to be 1. ϕ_{ij} are proper elements coresponding to ith node and jth mode.

ORIGINAL FILTER

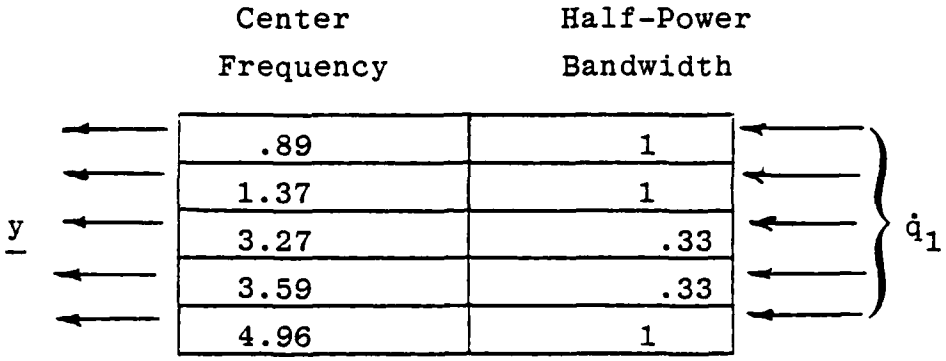

NEW FILTER

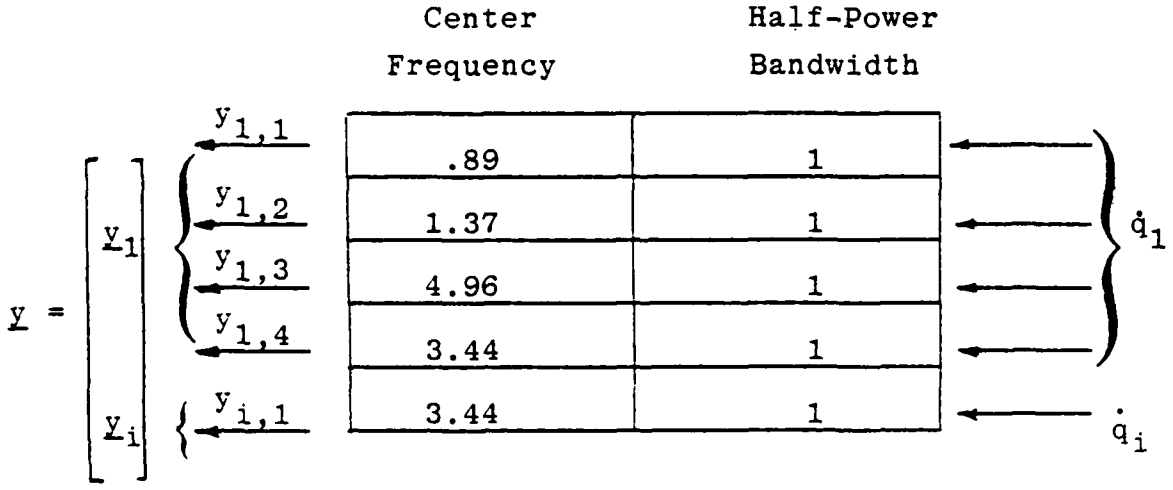

$\dot{q}_i$ is the velocity measurement from the second sensor placed at the ith node.

$\dot{q}_1$ is the velocity measurement from the 1st sensor located at the 1st node.

From equations (11) and (12)

$$\begin{bmatrix} \dot{\xi}_4 \\ \dot{\xi}_5 \end{bmatrix} = \begin{bmatrix} \phi_{1,4} & \phi_{1,5} \\ \phi_{i,4} & \phi_{i,5} \end{bmatrix}^{-1} \begin{bmatrix} y_{1,4} \\ y_{i,1} \end{bmatrix} \tag{13}$$

Thus, knowing $y_{1,4}$ and $y_{i,1}$, $\dot{\xi}_4$ and $\dot{\xi}_5$ can be estimated. Clearly, if the matrix

$$\begin{bmatrix} \phi_{1,4} & \phi_{1,5} \\ \phi_{i,4} & \phi_{i,5} \end{bmatrix}$$

is far away from being singular, resolution of $\dot{\xi}_4$ and $\dot{\xi}_5$ will be better. Hence, the location of the second sensor can be found by maximizing the determinent of the 2x2 matrix. Numerical calculations show that node 13 is best suited for this purpose.

The stability result is presented in Table 2. It contains the frequencies and the damping ratios of the structural and filter modes of a modified control system which has two sensors. The closed loop system is stable; however, the desired damping ($\zeta = 0.10$) is not obtained.

In order to have still better performance controlling 5 modes of the structure with velocity sensors, 6 velocity sensors could be located at different places. These sensors must have wide enough bandwidths to cover the 5 modes to be controlled and the one uncontrolled mode at a lower frequency. Then, a 6x6 spatial filter could be used to algebraically transform the sensor signals to the 6 lowest

TABLE 2

TWO SENSOR SYSTEM

ONE SENSOR AT NODE 1, THE OTHER SENSOR AT NODE 13

MODE TYPE	OPEN LOOP		CLOSED LOOP	
	ζ_r	f_r	ζ_r	f_r
SM1	.0430	.5840	.1406	.2335
SM2	.0500	.89	.0512	.8782
FM2	.5618	.89	.3931	1.3521
SM3	.035	1.37	.0198	1.32
FM3	.3642	1.37	.2721	2.5297
SM4	.01	3.279	.0072	2.8213
FM4	.1454	3.4396	.0653	3.9397
SM5	.009	3.593	.0867	3.1225
FM5	.1454	3.4396	.0504	4.3322
SM6	.013	4.957	.0873	3.8597
FM6	.1009	4.957	.0489	5.4714
SM7	.0035	5.485	.0063	5.488
SM8	.003	5.654	.0030	5.6540
SM9	.006	6.194	.0108	6.2311
SM10	.006	7.997	.0068	8.0283

SM_r - Denotes System Mode r

FM_r Denotes Filter Mode r

frequency modal velocities. In order that these sensors do not pick up the modal velocities of higher frequency modes, the sensors' signals should be sent through low pass temporal filters. The response of modes in the filters' roll-off region could be diminished by placing the sensors near the nodes of these potentially troublesome modes. This concept is pictured below.

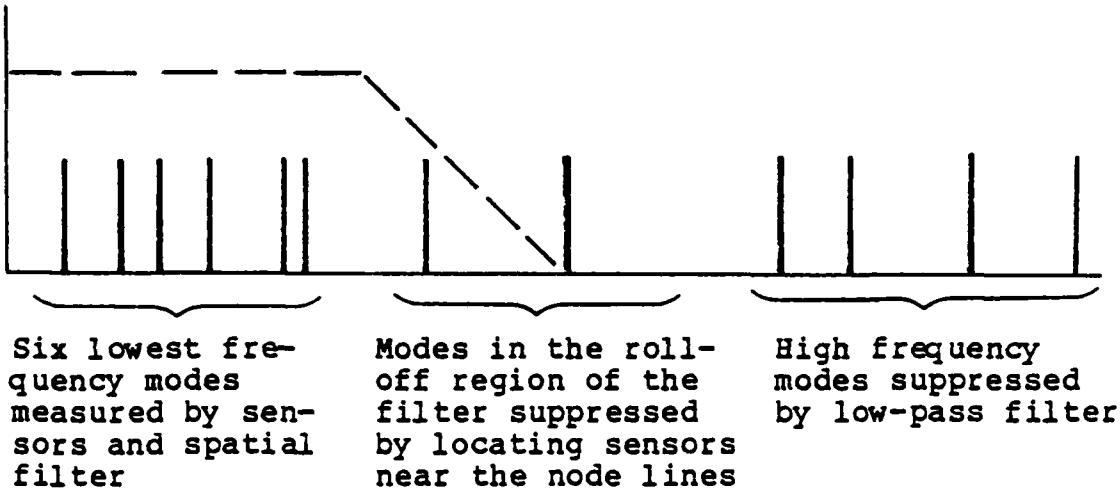

SIX SENSOR CONCEPT

CONCLUSION

It has been shown that the control apportioning matrix is an optimal solution to the Linear Quadratic Regulator problem. But, because of the test article filters, the closed loop system does not behave as expected. If a Kalman filter is implemented instead of the present filters, an improved result will be obtained.

The stability of the test article can be improved without many changes, by using a second sensor. An optimal location for the second sensor has been obtained, and the numerical analysis shows the stability of the closed loop system is improved. Further improvement in controlling 5 modes can be achieved by using 6 sensors and a low-pass filter. A brief description of this method has been provided.

REFERENCES

1. Hallauer, W.L., Jr., G.R.Skidmore, R.N. Gehling, "Modal-Space Active Damping of a Plane Grid: Experiment and Theory," presented at AIAA Dynamics Specialists Conference, May 17-18, 1984, Palm Springs, California, AIAA Paper No. 84-1018-CP.
2. Numerical modal data provided to HR Textron by VPI in April 1984. 56 degree of freedom model.

HR TEXTRON

APPENDIX C

DEVELOPMENT OF AN ALTERNATE CONTROL LAW FOR THE VPI PENDULOUS PLANE GRID

Arun P. Nayak, PhD

November 28, 1984

HR Textron Inc.
Systems Engineering Division
2485 McCabe Way
Irvine, California 92714

(714) 660-0253

DEVELOPMENT OF AN ALTERNATE CONTROL LAW FOR THE VPI PENDULOUS PLANE GRID

INTRODUCTION AND SUMMARY

This report develops alternate control and estimator laws to suppress vibration of the VPI pendulous plane grid. The controller and the estimator try to induce active damping in the first six modes of the test article with the help of five collocated actuators and sensors. The controller is developed independent of the estimator based on the principle of certainty equivalence, i.e., the controller is designed on the premise that the output of the estimator is the true value of the states that it is estimating. The controller and the estimator designs are based on the Model Error Sensitivity Suppression principle described in Reference [1].

The analysis shows that when these particular control and estimator laws are used, collocated actuators and sensors always induce active damping in almost all of the controlled and residual modes. Thus, the closed loop system is always stable. The analysis further shows that, for these particular control and estimator laws, the noncollocated actuators and sensors do not always guarantee stability for the closed loop system. Simulation results are given for only the collocated actuators and sensors, and they corroborate the analytical results.

A description of the test setup is given in Reference [2]. This analysis assumes that five velocity sensors are located at the same positions as the five actuators noted in Reference [2].

The section on Preliminaries sets up the general framework for the problem, and the sections on Control and Estimation Laws develop MESS-like control and estimation laws. The Closed Loop Analysis section derives the sufficiency condition for the stability of the closed loop system. The sections on Collocated Actuators and Sensors and Simulation Results contain the numerical results for the pendulous plane grid.

PRELIMINARIES

The dynamics of the pendulous plane grid are assumed to be given by

$$[M]\ddot{\underset{\sim}{x}} + [D]\dot{\underset{\sim}{x}} + [K]\underset{\sim}{x} = [B]\underset{\sim}{u} \qquad \ldots(1)$$

$$\dot{\underset{\sim}{y}} = [C]\dot{\underset{\sim}{x}} \qquad \ldots(2)$$

[M], [D], and [K] are mass, damping and stiffness matrices, respectively. $\underset{\sim}{x}$ represents the vector of physical displacements of the nodes. [B] and [C] are the control and the observation matrices, respectively. $\dot{\underset{\sim}{y}}$ is the observation vector, and $\underset{\sim}{u}$ is the control vector.

Equation (2) represents the fact that only velocity sensors are used.

The transformation between modal coordinates, $\underset{\sim}{q}$, and physical coordinates is

$$\underset{\sim}{x} = [\phi]\underset{\sim}{q} \qquad \ldots(3)$$

which has the following properties

$$[\phi^T]\,[M]\,[\phi] = [I] \qquad \ldots(4)$$

$$[\phi^T]\,[K]\,[\phi] = [\omega^2] \qquad \ldots(5)$$

[I] is an identity matrix. The columns of $[\phi]$ represent the mode shapes, and $[\omega^2]$ is a diagonal matrix whose diagonal elements are squares of the natural angular frequencies of the modes.

Using the above transformation, Equations (1) and (2) can be written as follows:

$$\ddot{q} + [2\zeta\omega]\,\dot{q} + [\omega^2]\,q = [\phi^T]\,[B]\,u \qquad \ldots(6)$$

$$\dot{y} = [C]\,[\phi]\,\dot{q} \qquad \ldots(7)$$

where $[2\zeta\omega] = [\phi^T]\,[D]\,[\phi]$ and is assumed to be diagonal. ζ is the damping ratio.

Define

$$[\phi_A] \triangleq [\phi^T]\,[B] \qquad \ldots(8)$$

and $$[\phi_o] \triangleq [C]\,[\phi] \qquad \ldots(9)$$

Equations (6) and (7) can be written in terms of the modes to be controlled and the residual modes (or left over modes)

$$\ddot{q}_c + [2\zeta\omega]_c\,\dot{q}_c + [\omega^2]_c\,q_c = [\phi_A]_c\,u \qquad \ldots(10)$$

$$\ddot{\underset{\sim}{q}}_\gamma + [2\zeta\omega]_\gamma \dot{\underset{\sim}{q}}_\gamma + [\omega^2]_\gamma \underset{\sim}{q}_\gamma = [\phi_A]_\gamma \underset{\sim}{u} \qquad \ldots(11)$$

$$\dot{\underset{\sim}{y}} = [\phi_o]_c \dot{\underset{\sim}{q}}_c + [\phi_o]_\gamma \dot{\underset{\sim}{q}}_\gamma \qquad \ldots(12)$$

The subscripts c and γ refer to the modes that are to be Controlled and to the Residual modes. Thus, $\underset{\sim}{q}_c$ refers to the modal coordinates of the modes to be controlled and $\underset{\sim}{q}_\gamma$ refers to the modal coordinates of the residual modes. The matrices $[2\zeta\omega]$, $[\omega^2]$, $[\phi_A]$, and $[\phi_o]$ are partitioned accordingly.

The purpose of the control $\underset{\sim}{u}$ is to induce active damping in controlled modes, i.e.,

$$[\phi_A]\ \underset{\sim}{u} = -[2\zeta_A\omega]_c\ \dot{\underset{\sim}{q}}_c \qquad \ldots(13)$$

where $[2\zeta_A\omega]_c$ is a diagonal matrix, and ζ_A is the desired active damping ratio.

Thus, the purpose here is to generate control $\underset{\sim}{u}$ which is as close to Equation (13) as possible and based on $\dot{\underset{\sim}{y}}$, the measurements.

CONTROL LAW

The following form for the control will be assumed

$$\underset{\sim}{u} = -[K_c]\ \dot{\underset{\sim}{q}}_c \qquad \ldots(14)$$

The control gain $[K_c]$ should have the following property:

$$[\phi_A]_c \; [K_c] = [2\zeta_A \omega]_c \qquad \ldots(15)$$

This will satisfy the Equation (13), the control requirement.

The control forces, will "spillover" into the residual modes. Thus, to suppress that, (this is the MESS principle, Reference [1]), $[K_c]$ should be

$$[\phi_A]_\gamma \; [K_c] = [0] \qquad \ldots(16)$$

Combining Equations (15) and (16) produces

$$[\phi_A] \; [K_c] = \begin{bmatrix} [2\zeta_A \omega]_c \\ [0] \end{bmatrix} \qquad \ldots(17)$$

$[K_c]$ can be obtained as a least square solution of Equation (17) as

$$[K_c] = \left\{ [\phi_A^T] \; [\phi_A] \right\}^{-1} [\phi_A^T] \begin{bmatrix} [2\zeta_A \omega]_c \\ [0] \end{bmatrix} \qquad \ldots(18)$$

It is assumed that the rank of ϕ_A is equal to the dimension of the control $\underset{\sim}{u}$.

The above control law may be obtained by the Linear Quadratic Regulator method by proper choices of weighting

matrices, as suggested in Reference [3].

ESTIMATION LAW

The following form for the estimate will be assumed.

$$\hat{\dot{q}}_c = [K_E]\ \dot{y} \qquad \ldots(19)$$

$\hat{\dot{q}}_c$ is the estimate of $\dot{q}_c$.
Substituting Equation (12) for $\dot{y}$, one obtains

$$\hat{\dot{q}}_c = [K_E]\ [\phi_o]_c\ \dot{q}_c + [K_E]\ [\phi_o]_\gamma\ \dot{q}_\gamma \qquad \ldots(20)$$

For a good estimate $[K_E]$ should be such that

$$[K_E]\ [\phi_o]_c = [I] \qquad \ldots(21)$$

where [I] is an identify matrix.

The term $[K_E]\ [\phi_o]_\gamma$ represents the observation spillover, and to suppress that a MESS-like approach will be used, i.e., one needs,

$$[K_E]\ [\phi_o]_\gamma = [0] \qquad \ldots(22)$$

Combining Equations (21) and (22), one gets

$$[K_E]\ [\phi_o] = \left[[I] \vdots [0]\right] \qquad \ldots(23)$$

$[K_E]$ can be obtained as a least square solution of Equation (23) as

$$[K_E] = \left[[I] \vdots [0]\right] [\phi_o^T] \quad \left\{ [\phi_o]\ [\phi_o^T] \right\}^{-1} \qquad \ldots(24)$$

It is assumed that the rank of $[\phi_o]$ is equal to the dimension of the observations $\underset{\sim}{y}$.

CLOSED LOOP ANALYSIS

From the implementation point of view, the control $\underset{\sim}{u}$ will be generated by

$$\underset{\sim}{u} = -[K_c]\ \hat{\underset{\sim}{q}}_c \qquad \ldots(25)$$

where $[K_c]$ is obtained from Equation (18) and $\hat{\underset{\sim}{q}}_c$ is obtained from Equations (19) and (24).

Substituting Equations (25), (19), (7) and (8) in Equation (6), produces

$$\ddot{\underset{\sim}{q}} + [2\zeta\omega]\ \dot{\underset{\sim}{q}} + [\omega^2]\ \underset{\sim}{q} = -\ [\phi_A]\ [K_c]\ [K_E]\ [\phi_o]\ \dot{\underset{\sim}{q}} \qquad \ldots(26)$$

Define

$$[2\zeta\omega]_I \triangleq [\phi_A]\ [K_C]\ [K_E]\ [\phi_O] \qquad \ldots(27)$$

The matrix $[2\zeta\omega]_I$ will dictate the stability of the closed loop system. If the matrix,

$$[2\zeta\omega]_M = [2\zeta\omega] + [2\zeta\omega]_I \qquad \ldots(28)$$

is positive definite, the closed loop system will be stable. For details see Appendix A.

In the case of collocated actuators and sensors, closed loop stability is assured for the above control and estimation laws. This is shown in the next section.

When actuators and sensors are not collocated, i.e., $[\phi_A^T] \neq [\phi_O]$, stability condition may not be satisfied. The system may be stable in two ways; (i) Change the locations of actuators and sensors, and/or (ii) change $[K_C]$ and $[K_E]$ in the following way:

$$[K_C] = \left\{[\phi_A^T]\ [Q_C]\ [\phi_A]\right\}^{-1}\ [\phi_A^T]\ [Q_C] \left[\frac{[2\zeta_A\omega]_C}{[0]}\right] \qquad \ldots(29)$$

and $$[K_E] = \left\{[I] \vdots [0]\right\}\ [Q_E]\ [\phi_O]^T\ \left\{[\phi_O]\ [Q_E]\ [\phi_O^T]\right\}^{-1} \qquad \ldots(30)$$

Equations (29) and (30) are generalized pseudo inverse solutions of Equations (17) and (23), respectively. The arbitrary matrices $[Q_C]$ and $[Q_E]$ must be positive—definite

and symmetric. They can be varied such that $[2\zeta\omega]_M$ is a positive definite matrix, thus stabilizing the closed loop system.

COLLOCATED ACTUATORS AND SENSORS

Collocation of actuators and sensors implies

$$[\phi_O] = [\phi_A^T] \qquad \ldots(31)$$

Simplifications occur in this special case. Equation (24) now can be written as

$$[K_E] = \left[[I] \vdots [0]\right] \; [\phi_A] \; \left\{[\phi_A^T] \; [\phi_A]\right\}^{-1} \qquad \ldots(32)$$

Equation (27) can now be written using Equations (31), (32) and (18) as

$$[2\zeta\omega]_I = [\phi_A] \left\{[\phi_A^T] \; [\phi_A]\right\}^{-1} [\phi_A^T] \left[\frac{[2\zeta_A\omega]_C}{[0]}\right] \left[[I] \vdots [0]\right] [\phi_A] \; x \qquad \ldots(33)$$

$$\left\{[\phi_A^T] \; [\phi_A]\right\}^{-1} \; [\phi_A^T]$$

$[2\zeta\omega]_I$ can be seen to be a positive semidefinite matrix. Since $[2\zeta\omega]$ is a positive definite matrix, $[2\zeta\omega]_M$ is a positive definite matrix. Thus, the closed loop system is stable.

The implication of $[2\zeta\omega]_I$ being positive semidefinite is that almost all the modes of the system can get active damping. Thus, the closed loop system is more robust than

the open loop system.

NUMERICAL ANALYSIS

The above problem of collocated actuators and sensors was numerically simulated using the data provided by VPI in Reference [4]. Five actuator-sensor pairs are placed at node locations 1, 4, 10, 13 and 22 of the dynamic model of the test article. The first 20 modes are used to model the dynamics of the test article. It is desired to provide active damping to the first six modes.

Figure (1) shows the schematic of the closed loop system.

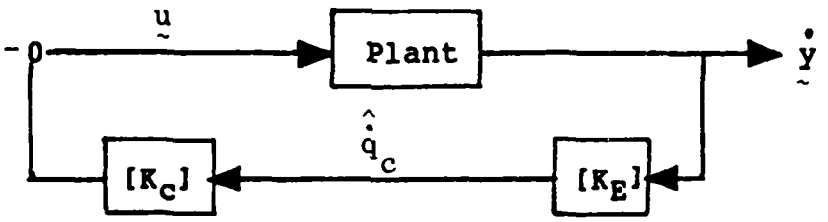

FIGURE 1

The control gain matrix $[K_C]$ and the estimation gain matrix $[K_E]$ were obtained using Equations (18) and (32), respectively.

Table 1 contains the open-loop eigenvalues and closed-loop eigenvalues for two cases. The results confirm the analytical observation that collocated actuators and sensors induce active damping in almost all system modes.

Active damping is provided only to the modes to be controlled when the controller is used without the estimator. When the estimator is also used, almost all the residual modes get some active damping, thereby showing that the compensator is trying to suppress the observation spillover. But this takes place at the expense of controlled mode damping, where the active damping predicted by the controller only is not achieved. But the overall closed-loop system is more robust than the open-loop system.

Table 2 contains the control gain matrices $[K_C]$ for both cases, and the estimation gain matrix $[K_E]$, which is the same in both the cases.

CONCLUSION AND DISCUSSION

MESS-like control and estimation laws are developed to control the first six modes of the VPI pendulous plane grid. A general case has been analyzed to study the stability of the closed-loop system. If the closed-loop system is found to be unstable, that can be remedied in two ways: (i) change

TABLE 1

SYSTEM PERFORMANCE

		CASE A*				CASE B*			
OPEN LOOP		CLOSED LOOP (NO ESTIMATOR)		CLOSED LOOP (WITH ESTIMATOR)		CLOSED LOOP (NO ESTIMATOR)		CLOSED LOOP (WITH ESTIMATOR)	
Frequency (Hz)	ζ	Frequency (Hz)	ζ	Frequency (Hz)	ζ	Frequency (Hz)	ζ	Frequency (Hz)	ζ
.58385	.043	.5848	.077	.5856	.109	.5849	.077	.5887	.153
.8898	.05	.8898	.081	.8897	.0077	.8899	.081	.8881	.084
1.3731	.035	1.3724	.104	1.3712	.1115	1.3734	.104	1.370	.137
3.2792	.01	3.2877	.0563	3.2859	.0354	3.3197	.102	3.3118	.0595
3.593	.009	3.582	.0556	3.5840	.0363	3.5469	.103	3.555	.0618
4.9572	.013	4.955	.0599	4.9557	.03667	4.950	.107	4.9526	.0594
5.4848	.0035	5.4848	.0035	5.4846	.004	5.485	.0035	5.484	.0044
5.6535	.003	5.6535	.003	5.6535	.0032	5.654	.003	5.6533	.0033
6.1941	.006	6.1941	.006	6.1938	.0085	6.1942	.006	6.193	.0105
7.9967	.005	7.9966	.005	7.9966	.0077	7.9966	.005	7.997	.0102
8.3988	.005	8.3988	.005	8.3970	.0098	8.3988	.005	8.3912	.0139
9.393	.005	9.393	.005	9.390	.0113	9.3930	.005	9.386	.0175
9.8065	.005	9.8065	.005	9.806	.0058	9.8065	.005	9.8052	.0065
11.634	.005	11.634	.005	11.634	.0059	11.634	.005	11.633	.0065
13.273	.005	13.273	.005	13.272	.0073	13.273	.005	13.27	.0095
20.556	.005	20.556	.005	20.556	.0050	20.556	.005	20.556	.0050
24.730	.005	24.729	.005	24.729	.0053	24.729	.005	24.73	.0054
26.959	.005	26.959	.005	26.958	.0054	26.959	.005	26.958	.0058
28.856	.005	28.854	.005	28.855	.0054	28.855	.005	28.85	.0057
30.748	.005	30.747	.005	30.747	.0052	30.747	.005	30.747	.0054

*

Case A: Desired active damping ratio in first six modes (.1, .1, .1, .1, .1, .1)

Case B: Desired active damping ratio in first six modes (.1, .1, .1, .2, .2, .2)

the actuator and sensor locations, and/or (ii) change the control gain and/or estimates gain using generalized pseudoinverses.

It has been shown that for collocated actuators and sensors, almost all modes - controlled and residual - can get some active damping; thus, the closed-system is always stable. The numerical simulation confirms this result.

The estimator developed here does not have any dynamics. This reduces complexity, on the other hand, there is no guarantee of closed-loop stability in the general situation. However, the system will be always stable when actuators and sensors are collocated. A Kalman filter may be advisable, but it will introduce estimator dynamics and complicate implementation somewhat.

TABLE 2

CONTROLLER AND ESTIMATOR MATRICES

Estimator gain matrix $[K_E]$

$$[K_E] = \begin{matrix} -1.3206D-02 & -1.6223D-02 & -1.0707D-02 & -8.3464D-03 & -1.1465D-02 \\ -3.8470D-05 & 6.1054D-03 & 1.7179D-02 & -3.0051D-03 & 1.5691D-02 \\ 2.4742D-02 & 1.9544D-02 & -1.5429D-02 & 1.4824D-02 & -1.3814D-02 \\ 1.5225D-02 & -8.5192D-03 & 1.6627D-02 & 1.6475D-02 & -5.9609D-03 \\ -8.2507D-03 & -2.3485D-02 & 5.3855D-03 & 1.8490D-02 & 1.4117D-02 \\ 2.0125D-02 & -2.5083D-03 & -7.2069D-03 & 2.0988D-03 & 2.2476D-02 \end{matrix}$$

Controller gain matrix $[K_c]$, Case 1

$$[K_c] = \begin{matrix} -9.6892D-03 & -4.3019D-05 & 4.2692D-02 & 6.2737D-02 & -3.7253D-02 & 1.2536D-01 \\ -1.1903D-02 & 6.8274D-03 & 3.3722D-02 & -3.5106D-02 & -1.0604D-01 & -1.5625D-02 \\ -7.8553D-03 & 1.9211D-02 & -2.6622D-02 & 6.8517D-02 & 2.4316D-02 & -4.4895D-02 \\ -6.1237D-03 & -3.3604D-03 & 2.5579D-02 & 6.7891D-02 & 8.3484D-02 & 1.3075D-02 \\ -8.4119D-03 & 1.7546D-02 & -2.3836D-02 & -2.4564D-02 & 6.3739D-02 & 1.4002D-01 \end{matrix}$$

$$[K_c] \times [K_E] = \begin{matrix} 4.9697D-03 & 1.0172D-03 & -6.1667D-04 & 1.3218D-03 & 1.4385D-03 \\ 1.0172D-03 & 3.7224D-03 & -1.3177D-03 & -1.9931D-03 & -1.8611D-03 \\ -6.1667D-04 & -1.3177D-03 & 2.4186D-03 & 1.0974D-03 & -3.1497D-04 \\ 1.3218D-03 & -1.9931D-03 & 1.0974D-03 & 3.1300D-03 & 7.3183D-04 \\ 1.4385D-03 & -1.8611D-03 & -3.1497D-04 & 7.3183D-04 & 4.8943D-03 \end{matrix}$$

Controller gain matrix $[K_c]$, Case 2

$$[K_c] = \begin{matrix} -9.6892D-03 & -4.3019D-05 & 4.2692D-02 & 1.8547D-01 & -7.4506D-02 & 2.5073D-01 \\ -1.1903D-02 & 6.8274D-03 & 3.3722D-02 & -7.0212D-02 & -2.1208D-01 & -3.1251D-02 \\ -7.8553D-03 & 1.9211D-02 & -2.6622D-02 & 1.3703D-01 & 4.8632D-02 & -8.9790D-02 \\ -6.1237D-03 & -3.3604D-03 & 2.5579D-02 & 1.3578D-01 & 1.6697D-01 & 2.6149D-02 \\ -8.4119D-03 & 1.7546D-02 & -2.3836D-02 & -4.9127D-02 & 1.2748D-01 & 2.8003D-01 \end{matrix}$$

$$[K_c] \times [K_E] = \begin{matrix} 8.7551D-03 & 1.0432D-03 & -6.7765D-04 & 1.9297D-03 & 3.3564D-03 \\ 1.0432D-03 & 6.5510D-03 & -2.3599D-03 & -4.5649D-03 & -3.5000D-03 \\ -6.7765D-04 & -2.3599D-03 & 4.0124D-03 & 2.5816D-03 & -1.3892D-03 \\ 1.9297D-03 & -4.5649D-03 & 2.5816D-03 & 5.8195D-03 & 1.7995D-03 \\ 3.3564D-03 & -3.5000D-03 & -1.3892D-03 & 1.7995D-03 & 9.0876D-03 \end{matrix}$$

APPENDIX A

Consider the linear time-invariant system

$$[A]\ \ddot{\underset{\sim}{x}} + [D]\ \dot{\underset{\sim}{x}} + [G]\ \dot{\underset{\sim}{x}} + [K]\ \underset{\sim}{x} = 0 \qquad \ldots(A.1)$$

where $\underset{\sim}{x}$ is a vector, [A] and [D] are symmetric, positive definite matrices, [K] is a symmetric matrix and [G] is a skew symmetric matrix.

The null solution of (A.1) will be asymtotically stable if all of the Eigenvalues of [K] are positive and unstable if [K] has at least one negative Eigenvalue.

This theorem is known as the Kelvin-Tait-Chataev theorem. For more details, see Reference [5].

Note that any matrix can be represented as the sum of a symmetric matrix and a asymmetric matrix, e.g.,

$$[E] = \frac{[E + E^T]}{2} + \frac{[E - E^T]}{2} \qquad \ldots(A.2)$$

Thus, positive definiteness of the matrix implies positive definiteness of the symmetric part.

REFERENCES

[1] Sesak, J. R., "Suppressed Mode Damping for Modal Error Sensitivity Suppression Flexible Spacecraft Controllers," Proceedings of the AIAA Guidance and Control Conference, 1980.

[2] Hallauer, W. L., Jr., Skidmore, G. R., and Gehling, R. N., "Modal-Space Active Damping of a Plane Grid Structure: Theory and Experiment," presented at the AIAA Dynamics Specialists Conference, Palm Springs, May 17-18, 1984, AIAA Paper 84-1018.

[3] Nayak, A., HR Textron Report, "Analysis of the VPI Active Structural Damping Experiment," July 18, 1984.

[4] Numerical modal data provided to HR Textron by VPI in April 1984, 56 degree of freedom model.

[5] Hefner, R. D., Hallman, W. P., "Space Structure Control via a Frequency-Shaped KTC Approach," paper presented at AAS/AIAA Astrodynamics Specialist Conference, Lake Tahoe, Nevada, 1981.

END

FILMED

3 -86

DTIC